Low-dose melittin is safe for intravitreal administration and ameliorates inflammation in an experimental model of uveitis

Brenda Fernanda Moreira Castro [a],[*], Carolina Nunes da Silva [a], Lídia Pereira Barbosa Cordeiro [b],
Sarah Pereira de Freitas Cenachi [c], Daniel Vitor Vasconcelos-Santos [c], Renes Resende Machado [a],
Luiz Guilherme Dias Heneine [d], Luciana Maria Silva [e], Armando Silva-Cunha [a], Silvia
Ligório Fialho [f]

[a] Faculty of Pharmacy, Federal University of Minas Gerais, 6627 Presidente Antônio Carlos Avenue, Pampulha, Belo Horizonte, Minas Gerais, 31270-901, Brazil
[b] Department of Chemistry, Federal University of Minas Gerais, 6627 Presidente Antônio Carlos Avenue, Pampulha, Belo Horizonte, Minas Gerais, 31270-901, Brazil
[c] Faculty of Medicine, Federal University of Minas Gerais, 190 Professor Alfredo Balena Avenue, Santa Efigenia, Belo Horizonte, Minas Gerais, 30130-100, Brazil
[d] Laboratory of Immunology, Ezequiel Dias Foundation, 80, Conde Pereira Carneiro Street, Gameleira, Belo Horizonte, Minas Gerais, 30510-010, Brazil
[e] Laboratory of Cell Biology, Ezequiel Dias Foundation, 80, Conde Pereira Carneiro Street, Gameleira, Belo Horizonte, Minas Gerais, 30510-010, Brazil
[f] Pharmaceutical Research and Development, Ezequiel Dias Foundation, 80, Conde Pereira Carneiro Street, Gameleira, Belo Horizonte, Minas Gerais, 30510-010, Brazil

ARTICLE INFO

ABSTRACT

Uveitis is a group of sight-threatening ocular inflammatory disorders, whose mainstay of therapy is associated with severe adverse events, prompting the investigation of alternative treatments. The peptide melittin (MEL) is the major component of *Apis mellifera* bee venom and presents anti-inflammatory and antiangiogenic activities, with possible application in ophthalmology. This work aims to investigate the potential of intravitreal MEL in the treatment of ocular diseases involving inflammatory processes, especially uveitis. Safety of MEL was assessed in retinal cells, chick embryo chorioallantoic membranes, and rats. MEL at concentrations safe for intravitreal administration showed an antiangiogenic activity in the chorioallantoic membrane model comparable to bevacizumab, used as positive control. A protective anti-inflammatory effect in retinal cells stimulated with lipopolysaccharide (LPS) was also observed, without toxic effects. Finally, rats with bacille Calmette-Guerin- (BCG) induced uveitis treated with intravitreal MEL showed attenuated disease progression and improvement of clinical, morphological, and functional parameters, in addition to decreased levels of proinflammatory mediators in the posterior segment of the eye. These effects were comparable to the response observed with corticosteroid treatment. Therefore, MEL presents adequate safety profile for intraocular administration and has therapeutic potential as an anti-inflammatory and antiangiogenic agent for ocular diseases.

1. Introduction

The ocular immune-privilege, endowed with multiple and specialized components, protects the eye through functional and structural mechanisms that maintain its integrity and homeostasis (Hove et al., 2016). Inflammatory processes within the eye affect the integrity of ocular structures and fluids and, thus, are detrimental to vision function (Caspi, 2010). Hence, intraocular inflammation is the third leading cause of blindness in the world, accounting for 15% of preventable vision loss worldwide, and 25% of irreversible blindness in developing countries (Foster et al., 2016). Uveitis comprises a variety of ocular inflammatory disorders affecting the uvea and adjacent structures (de Smet et al., 2011). It affects mostly young individuals in their working years, causing an important economic and social burden (Chen et al., 2017; Fukunaga et al., 2020). Uveitis can be infectious or non-infectious according to etiology and can also be further classified regarding the primary anatomical site of inflammation, clinical course, and histopathology

Abbreviations

MEL	Melittin
LPS	lipopolysaccharide;
STAT	activator of transcription
ERK	extracellular signal-regulated kinase ½
JNK	c-jun N-terminal kinase
iNOS	inducible nitric oxide synthase
ARPE-19	human retinal pigmented epithelium cell line;
MTT	3-(4,5-dimethylthiazol-2-yl)-2,5-diphenyltetrazolium bromide;
FBS	fetal bovine serum
ICCVAM	Interagency Coordinating Committee on the Validation of Alternative Methods
CAM	chorioallantoic membrane
IS	irritation score
SD	standard deviation
IVT	intravitreal
IOP	intraocular pressure (IOP)
ERG	electroretinogram
ISCEV	International Society for Clinical Electrophysiology of Vision
FITC	fluorescein Isothiocyanate
BCG	Bacille Calmette-Guérin
DEX	dexamethasone sodium phosphate
NAG	N-acetylglucosaminidase
MPO	myeloperoxidase
OD	optical density
ELISA	enzyme-linked immunosorbent assay
ANOVA	analysis of variance
GCL	ganglion cell layer
IPL	inner plexiform layer
INL	inner nuclear layer
OPL	outer plexiform layer
ONL	outer nuclear layer
PRL	photoreceptor layer
RPE	retinal pigment epithelium cells
HUVEC	human umbilical vein endothelial cells
VEFG	vascular endothelial growth factor
TLR4	toll-like receptor 4
MD-2	myeloid differentiation protein-2
Akt	protein kinase B

(Foster et al., 2016; Gamalero et al., 2019). Management of non-infectious uveitis is challenging, since corticosteroids, the mainstay of therapy, are associated with severe adverse events after local and systemic administration. This is particularly observed in long-term treatment for chronic non-infectious uveitis, for which alternative corticosteroid-sparing/immunomodulatory therapies may be required in a significant number of patients for sustained control of intraocular inflammation (Rosenbaum et al., 2019). Once there is still a critical unmet need for effective and safe therapeutic options for uveitis, several studies have been investigating alternative treatments with numerous clinical trials underway (Hassan et al., 2019; Rosenbaum et al., 2019; Ahmed et al., 2020).

Melittin (MEL) is the major component of *Apis mellifera* bee venom, accounting for 50–60% of its dry weight (Pascoal et al., 2019). It is a linear amphiphilic peptide of 2840 Da, composed of 26 amino acids residues (GIGAVLKVLTTGLPALISWIKRKRQQ), in which the amino-terminal region is predominantly hydrophobic and the c-terminal is hydrophilic (Moreno and Giralt, 2015; Santos-Pinto et al., 2018). A wide spectrum of pharmacological effects has been described for MEL, including anticancer, antimicrobial, antiviral, antinociceptive, and anti-inflammatory (Rady et al., 2017; Wehbe et al., 2019; Aufschnaiter et al., 2020). As an anti-inflammatory agent, MEL has demonstrated a potent activity, being explored in different settings, including acne vulgaris, neuroinflammation, atopic dermatitis, atherosclerosis, rheumatoid arthritis, liver inflammation, and renal fibrosis (An et al., 2016; Lee and Bae, 2016; Kim et al., 2017; Pascoal et al., 2019). In inflammatory acne vulgaris and acute hepatic failure models MEL was able to decrease production of proinflammatory cytokines through regulation of the NF-κB signalling pathway (Lee et al., 2014). Similarly, in a model of atopic dermatitis, MEL decreased expression of proinflammatory mediators by suppressing NF-κB and signal transducer and activator of transcription (STAT) pathways (Kim et al., 2017; An et al., 2018). In microglial cells, MEL suppressed activation of NF-κB and inhibited phosphorylation of p38, extracellular signal-regulated kinase ½ (ERK ½), and c-jun N-terminal kinase (JNK) along with expression of inducible nitric oxide synthase (iNOS) (Moon et al., 2007). Although the potential of MEL as an anti-inflammatory agent has been evidenced in a variety of cell lines and animal models, it has not been explored for treatment of ocular diseases. Therefore, this work aims to establish a safety profile for intravitreal administration of MEL and to investigate the anti-inflammatory and antiangiogenic effects of MEL in vitro and in vivo.

2. Materials and methods

2.1. Animals

Male Wistar rats (n = 66) aged 6–8 weeks and weighing 180–220 g were used in this study. They were housed and maintained in the animal facility of the Pharmacy School of Universidade Federal de Minas Gerais, under controlled temperature (27 ± 5 °C) and luminosity (12h light/12h dark). Food and water were supplied *ad libitum* and the studies were conducted following the guide for the care and use of laboratory animals (National Institutes of Health Publications No. 8023, revised 1978) and in accordance with the Association for Research in Vision and Ophthalmology Resolution Standards for Animal Research. The study was approved by the Animal Ethics Committee of UFMG, under the protocol nº 303/2019.

Animals were randomly divided into 4 groups for the toxicity study (n = 4/group) and evaluation of retinal penetration (n = 2/group). To assess in vivo anti-inflammatory effect of MEL, 42 rats were divided into 7 groups (n = 6/group). At the end of each experiment, all animals were euthanized with an intraperitoneal injection of 270 mg/kg of ketamine (Dopalen, Ceva, Brazil) and 30 mg/kg of xylazine (Anasedan, Ceva, Brazil).

2.2. Cell culture and treatment

Human retinal pigmented epithelium cell line (ARPE-19) obtained from the American Type Culture Collection (ATCC CRL-2302, USA), was used in this study. The cells (passage 23) were cultured in a mixture (1:1) of DMEM and Ham's F-12 (DMEM/F-12; Sigma-Aldrich, USA), supplemented with 10% fetal bovine serum (FBS), and 1% antibiotics/antimycotic solution (100 units/mL penicillin, 100 μg/mL streptomycin and 0.25 μg/mL amphotericin B; Gibco, USA), at 37 °C in a humidified 5% CO_2 incubator.

2.3. MEL isolation from Apis mellifera bee venom

MEL was purified from *Apis mellifera* bee venom using heparin-affinity chromatography (HiPrep Heparin Fast Flow 16/10; GE healthcare, Brazil) in a GE AKTA Purifier 100 fast protein liquid chromatography system with UV-900 detector, as previously described by Banks et al. (1981). The peptide was desalted by solid-phase extraction

(SEK-PAK C18; Waters, Brazil), freeze-dried (ModulyoD, Thermo Scientific, USA), and stored at $-20\,°C$ in sealed lo-bind tubes. The purity (92.4 $\pm$ 7.4%) and identity (m/z of 2845.7) of MEL samples were assessed by high-performance liquid chromatography (HPLC, Agilent 1100, Agilent, USA) and MALDI-TOF/TOF (Autoflex III TOF/TOF 200, Bruker, Germany) analysis (data not shown). The latter was performed over alpha-cyano-4-hydroxycinnamic acid matrix, at 0–200 kDa m/z range, with data acquisition and analysis being carried out in the FlexControl 3.3 software. The liquid chromatographic method described by Haghi et al. (2013) was used to analyze the samples in a Shim-pack VP-ODS (250 mm x 4,6 mm x 5,0 μm) chromatographic column (Shimadzu, Japan). For in vitro and in vivo assays, a stock solution of MEL was prepared in sterile saline and diluted in culture medium (cell studies) or sterile saline (in vivo studies and CAM assays).

2.4. Cell viability by MTT

The viability of ARPE-19 cells treated with MEL was determined by the MTT (3-(4,5-dimethylthiazol-2-yl)-2,5-diphenyltetrazolium bromide) assay. Firstly, ARPE-19 cells were seeded at 1×10^4 cells/well in 96-well plates and incubated at 37 °C for 24 h. Later, the cells were treated with MEL solutions with increasing concentrations (0.5; 1.0; 1.5; 2.0; 2.5 and 3.0 μg/mL) prepared in DMEM/F-12 supplemented with 1% FBS. The same medium was used to prepare hydrogen peroxide solution (1 mM), which was used as the positive control. After 24, 48, and 72 h, the medium was replaced with 0.5 mg/mL MTT solution (Sigma-Aldrich, USA) and the plates were incubated for 3 h under the same conditions. Then, the precipitated formazan crystals were solubilized by adding dimethyl sulfoxide (Vetec, Brazil) and the optical densities were measured at 550 nm using a microplate reader (Spectramax 190; Molecular devices LCC, USA). Cell viability was reported as a percentage of control (untreated) viability. Data were obtained from three independent experiments.

2.5. Hen's egg test-chorioallantoic membrane (HET-CAM)

HET-CAM is an in vitro assay alternative to the Draize rabbit eye test. In this work, the HET-CAM assay was performed according to the protocol established by the Interagency Coordinating Committee on the Validation of Alternative Methods (ICCVAM) ICCVAM 2010), to evaluate the ocular tolerance of MEL. For this, viable fertilized hens' eggs (*Gallus gallus domesticus*), supplied by Granja Rivelli, (Minas Gerais, Brazil), were incubated for 9 days at 37 $\pm$ 0.5 °C and 55 $\pm$ 5% of relative humidity (Premium Ecológica, Brazil). On day 9, the eggshells were opened with surgical tweezers and the inner membrane was removed for exposure of the chorioallantoic membrane (CAM). A volume of 300 μL of MEL solution (0.1; 0.5; 1.0; 2.0; 2.5; 3.0 μg/mL), 0,1 M NaOH (positive control) or sterile saline (negative control) were applied onto the CAM surface. Throughout 5 min, blood vessels of the membrane were observed using a stereomicroscope (SZ61, Olympus, USA), in order to detect reactions as lysis, hemorrhage, and coagulation. The time onset for each reaction was recorded and photographs were taken after 0.5, 2, and 5 min with a digital camera attached to the microscope. The irritation score (IS) was calculated by the sum of the numerical scores (Table 1), and the classification of ocular irritation potential was determined as described in

Table 1
Numerical scores and ocular irritation classification for HET-CAM assay.

Effect	Score			IS	Classification
	0.5 min	2 min	5 min	0.0 to 0.9	non-irritant
Lysis	5	3	1	1.0 to 4.9	slight irritant
Hemorrhage	7	5	3	5.0 to 8.9	moderate
Coagulation	9	7	5	9.0 to 21.0	severe irritant

IS: Irritation score.

Table 1. The results were expressed as mean $\pm$ standard deviation (SD), n = 6 eggs/group.

2.5.1. Intravitreal injections

Prior to intravitreal (IVT) injections, the animals were anesthetized with intraperitoneal ketamine (80 mg/kg; Dopalen, Ceva, Brazil) and xylazine (10 mg/kg; Anasedan, Ceva, Brazil) followed by topical instillation of 0.1% phenylephrine/1% tetracaine eyedrops (Anestésico, Allergan, Brazil). A volume of 5 μL was injected through the pars plana of the right eyes with a 31-gauge needle (BD Ultrafine II, USA) inserted about 2 mm posterior to the limbus. The needle remained in place for about 30 s in order to prevent reflux when it was removed.

2.6. In vivo safety

The in vivo safety of MEL was assessed by ophthalmic examination, measurement of intraocular pressure (IOP), electroretinographic exams, and histopathological analyses. A total of 16 rats were randomly divided into 4 groups that received an IVT injection of MEL solution (0.5, 1.0, and 2.0 μg/mL) or vehicle (sterile saline) in their right eyes. Ophthalmic examinations and IOP measurements were conducted before, 6, and 14 days after IVT injections. The clinical examination consisted of indirect ophthalmoscopy (Eyetec, Brazil) employing a 90D wide-field noncontact lens (Volk Digital Wide Field, Volk, Germany) after pupillary dilation with 1% tropicamide drops (Mydriacyl, Alcon, USA). Fundus images were registered with a smartphone camera coupled to the 90D lens. IOP was measured with a TonoPen Vet (Reichert, USA) calibrated before each use. Measurements were taken under sedation with intraperitoneal ketamine/xylazine 80:10 mg/kg, and topical anesthesia with 0.1% phenylephrine/1% tetracaine. Each IOP value was an average of three consecutive readings taken in each eye, with a standard error $< 10\%$, and at the same conditions to avoid circadian variation.

Electroretinogram (ERG) recordings were carried out as reported by Toledo et al. (2019), 7 and 15 days after the IVT injections. Animals were dark-adapted for 12h and then sedated with intraperitoneal ketamine and xylazine (80:10 mg/kg). Pupils were dilated with topical tropicamide 1% and eyes were anesthetized with 0.1% phenylephrine/1% tetracaine eye drops. Subcutaneous reference electrodes were inserted near the temporal canthus of the animals' eyes while the ground electrode was inserted in the animals' rump. ERG responses were acquired using a corneal bipolar contact lens electrode (ERG Jet, Fabrinal SA, Switzerland) under dim red light. The full-field ERG was obtained in an Espion E2 electrophysiology system (Diagnosys LLC, USA) with a Ganzfeld LED stimulator (ColorDome desktop Ganzfeld, Diagnosys LLC, USA). The protocol was conducted following the guidelines of the International Society for Clinical Electrophysiology of Vision (ISCEV) (Robson et al., 2018). For the scotopic dark-adapted exam, white flashes of 6500 K and 4 ms of duration were delivered in 11 steps of increasing luminance intensity (0.003–3 cd.m.s^{-1}). The stimulus of 0.01 and 3 cd.m.s^{-1} were analyzed to evaluate rod and combined rod and cone responses, respectively. Next, the rats were light-adapted for 10 min under a background luminance of 3 cd.m.s^{-1} for the photopic exam. Flashes of 3 cd.m.s^{-1} for 4 ms followed by a 30-Hz flickering stimulus with the same luminance and duration were applied. The results were amplified and analyzed using the Espion E3 software (Diagnosys LLC, USA), and amplitudes and implicit times of a- and b-waves were measured as described by Chen et al. (2013). The effect of MEL on both response components was assessed by determining the mean $\pm$ SD percentage relative to the control group (vehicle) for each parameter and time-point.

After the last ERG examination, the animals were euthanized and their eyes enucleated for histopathological analysis. The eyes were fixed in Davidson's fixative solution, transferred to 70% ethanol, processed, embedded in paraffin blocks, sectioned through the sagittal plane (5 μm), and stained with hematoxylin-eosin for light microscopy analysis (Axio Imager M2 optic microscope, Zeiss, Germany).

2.7. Retinal penetration

MEL was conjugated with fluorescein Isothiocyanate (FITC, Sigma-Aldrich, USA), according to the protocol described by Maeda and Kawauchi (1968), to evaluate the location of the peptide in rats' retina after the IVT injection, at different time-points. The animals received an IVT injection of the conjugated peptide (MEL-FITC, 2 μg/mL) or FITC solution (n = 4/group), and were euthanized 2 or 8 h later (n = 2 per time-point). The eyes were enucleated for preparation of histology slides, which were analyzed by fluorescence microscopy at an excitation wavelength of 495 nm and an emission wavelength of 517 nm (Axio Vert-A1 FL-LED fluorescence microscope, Zeiss, Germany). A control slide from the vehicle group (saline) was used to adjust the background and mitigate retinal autofluorescence.

2.8. Antiangiogenic activity

Antiangiogenic activity of MEL was assessed by the chicken embryo CAM assay, as previously described by Vieira et al. (2020). Briefly, fertilized hens' eggs (*Gallus gallus domesticus*) incubated at 37 ± 0.5 °C and $55 \pm 5\%$ of relative humidity were opened on the 3rd day after fertilization and their inner membrane was removed for CAM exposure. On the 5th and 6th day, 50 μL of MEL solution (0.5, 1.0, and 2.0 μg/mL), sterile saline (negative control) or bevacizumab (Avastin, Roche, USA; positive control; 5 mg/mL) were applied on the CAM (n = 12/group) at a standardized location. The eggs were sealed and incubated afterward. On the 7th day, the membranes were photographed with a camera coupled to a stereomicroscope (SZ61, Olympus, USA), and the vascularized area was quantified using the ImageJ program, version 1.50i. The results were expressed as a percentage of the negative control group (100%).

2.9. In vitro anti-inflammatory activity

The effect of pre-treatment with MEL on LPS-induced inflammatory response in ARPE-19 cells was investigated by measuring the levels of inflammatory mediators in cells supernatant after LPS stimulus. ARPE-19 cells were cultured in complete medium in 96-well plates until reaching 80–90% of confluency. Then, cells were pre-treated with MEL (0.5, 1.0 and 2.0 μg/mL in serum-free medium) for 1 h followed by treatment removal and activation with LPS 10 μg/mL (*Escherichia coli*, serotype O111:B4; Sigma-Aldrich, USA) in serum-free medium for 24 h (n = 4/group). Phenol red-free medium (Gibco, USA) was used for nitrite determination and the chosen concentration of LPS was based on previous studies using the same cell-line (Leung et al., 2009; Arjamaa et al., 2017).

Next, cells supernatant was collected and levels of proinflammatory cytokines (IL-6, IL-8, IL-1β, TNF-α, INF-γ, IL-17A, TGF-β1) and nitrite were determined by flow cytometry and Griess reagent assay (Sigma-Aldrich, USA), respectively. A customized human inflammation panel (LEGENDPlex; Biolegend, USA) was used for flow cytometry analysis, which was performed according to the manufacturer's instructions in an LSRFortessa (BD Biosciences, USA) flow cytometer. Each sample and standard were assayed in duplicate and analyzed using Biolegend LEGENDplex data analysis software, as previously reported (Lehmann et al., 2019). Standard curves ranging from 10,000 to 2.44 or 20,000–4.88 pg/mL (TGF-β1) were used in the analysis ($R^2 > 0.99$). Nitric oxide (NO) levels were determined indirectly by measuring the nitrite concentration, using the modified Griess methodology described by da Silva et al. (2020). Samples were assayed in triplicate and the concentration of nitrite was determined by using a calibration curve (1–100 μM; R^2 0.999).

The following controls were also analyzed: Cells treated with MEL 2 μg/mL without LPS-activation (received medium instead), cells treated with medium followed by LPS-activation (untreated LPS-activated cells), and cells receiving medium only without LPS-activation (control).

2.10. In vivo anti-inflammatory activity

2.10.1. Induction of uveitis and treatment with MEL

The anti-inflammatory effect of MEL in vivo was assessed in rats using the animal model of uveitis induced by Bacille Calmette-Guérin (BCG), as previously described (Castro et al., 2020). First, the animals (n = 35) received on their dorsum a subcutaneous injection of BCG (2.6 mg/mL; (ImunoBCG 40 mg, equivalent to $>2.0 \times 10^6$ CFU/mg; Fundação Ataulpho de Paiva, Brazil) suspended in phosphate buffer and emulsified with mineral oil (Montanide ISA50 V2, Seppic, France). A second subcutaneous injection of the antigen was given after 7 days (day 8) and an intravitreal injection (5 μL) of BCG suspended in sterile saline (2 mg/mL) was given on day 15. IVT injections were performed as previously described for the in vivo safety study. After 3 days (day 18) the animals were randomly divided into 5 groups (n = 7/group) and received MEL solution (0.5, 1, and 2 μg/mL), dexamethasone sodium phosphate (DEX; Decadron solution for injection, 4 mg/mL) or sterile saline (vehicle) intravitreally. A group of healthy animals (n = 7) not submitted to any intervention was used as a control. The experimental design used for this study is illustrated in Fig. 1.

2.10.2. Ophthalmic evaluation

Ophthalmic examination was performed 2 days after intravitreal injection of BCG (day 17) and 6 days after treatment (day 24). In a masked fashion, an ophthalmologist examined all the animals and documented the observations. Slit-lamp biomicroscopy (Apramed HS5, Brazil) and indirect ophthalmoscopy (Eyetec, Brazil) employing a widefield noncontact lens (Volk Digital Wide Field, Volk, Germany) were performed after pupillary dilation with tropicamide 1%. Scoring of clinical findings was based on human standards for ocular inflammation (Standardization of Uveitis Nomenclature Working Group, 2005).

2.10.3. Electroretinography

Full-field electroretinographic exams were performed in 4 animals of each group at baseline, 3 days after the induction of uveitis, and 7 days after treatment, to evaluate the disease progression and treatment effect on retinal function. Scotopic and photopic exams were carried out as described in the in vivo safety study.
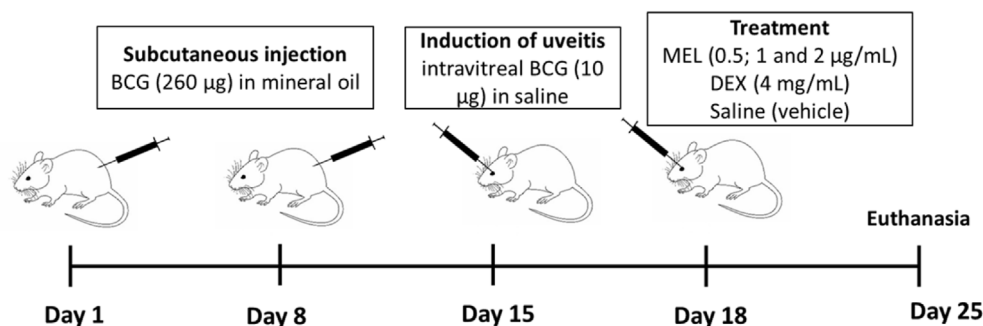

Fig. 1. Scheme of uveitis induction and intravitreal treatments. Rats were intraperitoneally inoculated with BCG on days 1 and 8 and the disease was induced on day 15 with an intravitreal injection of BCG. On day 18 the animals received an intravitreal injection of the following treatments: melittin 0.5, 1 and 2 μg/mL; dexamethasone sodium phosphate 4 mg/mL and saline. The healthy group was not submitted to any intervention and all animals were euthanized on day 25. BCG: bacille Calmette Guerin; MEL: melittin; DEX: dexamethasone sodium phosphate.

2.10.4. Histopathological analysis

All animals were euthanized 7 days after treatment (day 25) for histopathological evaluation and quantification of inflammatory markers. For histopathology, eyes of 3 animals (n = 3) were enucleated and processed as previously described in the safety study. Signs of inflammation on the anterior chamber, vitreous cavity, and retina were assessed by light microscopy.

2.10.5. Quantification of pro-inflammatory markers

The quantification of pro-inflammatory markers in ocular tissues was performed in 4 animals of each group after euthanasia. For this, eyes were enucleated and tissues of the posterior segment (sclera, choroid, and retina) were harvested, weighed, and homogenized in phosphate buffer containing Tween-20 (0.05%), phenylmethylsulphonyl fluoride (0.1 mM), benzethonium chloride (0.1 mM), EDTA (10 mM), aprotinin A (2 μg/mL) and bovine serum albumin (0.5%). Next, samples were centrifuged (10.000 rpm, 15 min, 4 °C) and the supernatant was collected for cytokines and nitrite quantification. The remained pellets were used to characterize the inflammatory infiltrate, by measuring the activity of N-acetylglucosaminidase (NAG) and myeloperoxidase (MPO). NAG is an enzyme present in high levels in activated macrophages, whereas MPO is produced by neutrophils (de Souza et al., 2012; Arafat et al., 2014). The assays were carried out according to the methodology described in Castro et al. (2020) using 3,3′–5,5′-tetramethylbenzidine (Sigma-Aldrich, USA) and 4-Nitrophenyl N-acetyl-β-D-glucosaminide (Sigma-Aldrich, USA) as substrates to determine MPO and NAG activity, respectively. Results were expressed as optical density (OD) per 100 mg of tissue.

Nitric oxide levels in posterior segment tissues were determined indirectly by measuring nitrite concentration in the homogenate supernatant, using the modified Griess reagent method (Sigma-Aldrich, USA). The assay was performed following the manufacturer's instructions and the result was reported as the concentration of nitrite per 100 mg of tissue, determined using a calibration curve (0.5–20 μM; $R^2 = 0.996$). Similarly, levels of IL-6, IL-1β, TNF-α, and CXCL-1 were determined in the posterior segment tissues by enzyme-linked immunosorbent assay (ELISA). The assay was carried out according to the manufacturer's instructions (DuoSet kits, R&D Systems, USA) at 490 nm. All samples were analyzed in duplicate and the results were expressed as pg/100 mg of tissue.

2.11. Statistical analysis

For the MTT assay, within each exposure time, all concentrations were compared to the negative control by unpaired *t*-test followed by Sidak-Bonferroni post-hoc test. Differences in cell viability between the exposure times were compared by two-way ANOVA with post-hoc Tukey for multiple comparisons. ERG and IOP data were compared by two-way ANOVA with Bonferroni as post-hoc test while all other results were compared by one-way ANOVA followed by post-hoc Bonferroni. GraphPad Prism 6 software (GraphPad Software Inc., USA) was used for the analysis, and $p < 0.05$ was considered to be statistically significant. Data were expressed as mean ± SD.

3. Results

3.1. The effect of melittin on the viability of ARPE-19 cells

ARPE-19 cells were treated with different concentrations of MEL (0.5; 1.0; 1.5; 2.0; 2.5 and 3.0 μg/mL) during 24, 48 and 72h. The concentrations of 0.5, 1, and 1.5 μg/mL did not affect cell viability compared to the control group, in all exposure times (Fig. 2A). MEL solution at concentrations of 2 μg/mL and above significantly reduced viability of ARPE-19 cells after 24h of treatment (p < 0.0001). The same behavior was observed after 48h of exposure (p < 0.0001), except for cells treated with MEL 2 μg/mL. However, this effect was not observed in cells treated with MEL for 72h, whose viability in all concentrations was not statistically different from the control cells. In fact, viability of ARPE-19 cells exposed to MEL for 72h was significantly higher (p < 0.0001) compared to 24 and 48h of exposure, for concentrations ≥1.5 and 2.0 μg/mL, respectively. There was no significant difference between 24 and 48h of treatment.

3.2. Ocular tolerance of MEL by HET-CAM assay

In HET-CAM assay, the potential of ocular irritation of a substance is assessed by detecting signs as hemorrhage, lysis and, coagulation on the CAM. All three signs of vascular response were observed within 30 s in the positive control group, 0.1 M NaOH (Fig. 2B), leading to a total score of 20.0 ± 1.1, indicative of a severe irritant agent (Fig. 2C). The negative
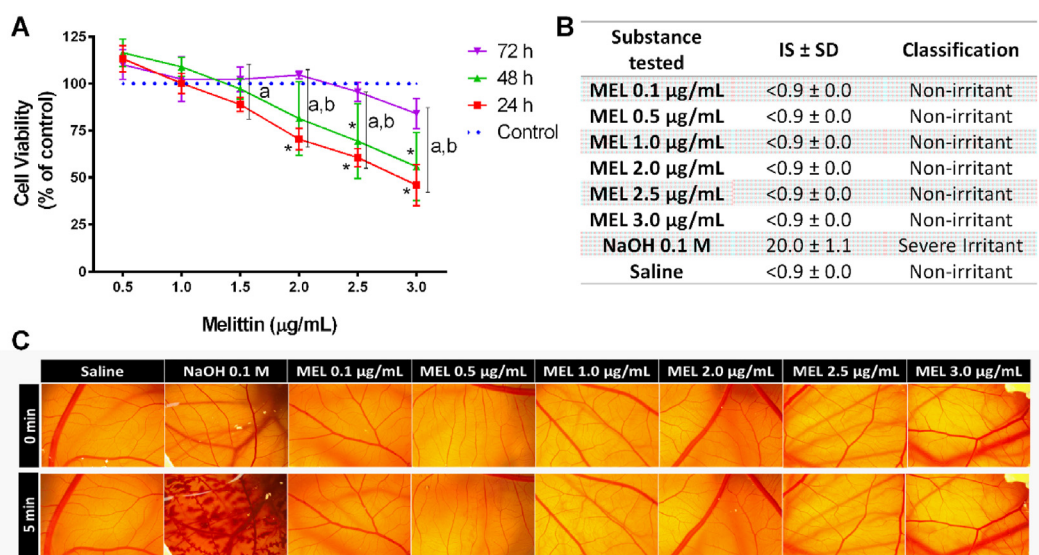

Fig. 2. Effect of melittin on the viability of ARPE-19 cells and the vascular network of chicken embryos chorioallantoic membrane. (A) MTT assay performed on ARPE-19 cells 24, 48, and 72h after exposure to melittin 0.5–3.0 μg/mL showed that concentrations up to 1.5 μg/mL did not affect cells viability at all time-points evaluated. (B) Representative stereomicrographs showing no signs of vascular response on chick embryos chorioallantoic membranes after administration of melittin 0.1–3.0 μg/mL and saline (negative control), while the positive control (0,1 M NaOH) presented expected reactions. (C) Cumulative irritation scores and ocular irritation classification for melittin and controls according to HET-CAM assay, n = 6/group. Data are mean ± SD, n = 3; *p < 0.05 compared with control. [a] p < 0.05 for 24 vs 72h; [b] p < 0.05 for 48 vs 72h. IS: irritation score; MEL: melittin.

Substance tested	IS ± SD	Classification
MEL 0.1 μg/mL	<0.9 ± 0.0	Non-irritant
MEL 0.5 μg/mL	<0.9 ± 0.0	Non-irritant
MEL 1.0 μg/mL	<0.9 ± 0.0	Non-irritant
MEL 2.0 μg/mL	<0.9 ± 0.0	Non-irritant
MEL 2.5 μg/mL	<0.9 ± 0.0	Non-irritant
MEL 3.0 μg/mL	<0.9 ± 0.0	Non-irritant
NaOH 0.1 M	20.0 ± 1.1	Severe Irritant
Saline	<0.9 ± 0.0	Non-irritant

control, saline, did not cause any vascular alteration on the CAM, being classified as non-irritant (score <0.9). Likewise, no changes on the CAM were noticed after applying all tested concentrations of MEL, which was categorized as non-irritant (score <0.9). It indicates that MEL 0.1–3.0 μg/mL is likely a non-irritant substance for ocular application, by the HET-CAM assay.

3.3. Melittin is safe for intraocular administration

Ophthalmic and ERG examinations, IOP monitoring, and histopathological analyses were performed to assess in vivo ocular safety of intravitreal MEL at 0.5, 1, and 2 μg/mL in rats. IOP of animals treated with intravitreal MEL was not significantly different from vehicle-treated group (saline) in all time-points and concentrations evaluated (p > 0.05) (Fig. 3A). Also, no fundus alterations were observed on indirect

ophthalmoscopy 6 and 14 days after intravitreal injections of MEL or vehicle (Fig. 3C). Fundus examination, thus, evidenced no signs of retinal toxicity, including hemorrhage, vascular changes or vitreous opacities, and showed a preserved optic disc in all groups evaluated. This was confirmed by the histopathological analysis (Fig. 3B), which showed no apparent retinal toxicity with absence of signs of inflammation or degeneration. These results were consistent with the electroretinographic evaluation, which revealed no significant difference in a- and b-waves mean amplitudes when compared to the vehicle group, in all time-points and flash intensities (Fig. 3D). This was observed in both scotopic and photopic exams and included the 30 Hz flicker evaluation (Fig. 3D). In addition, no remarkable changes were observed in the mean ERG curves (Fig. 3E) of all MEL groups. However, animals treated with MEL 2 μg/mL presented a significantly shorter implicit time for b-wave and flicker in the light-adapted exam performed 7 days after the injections,
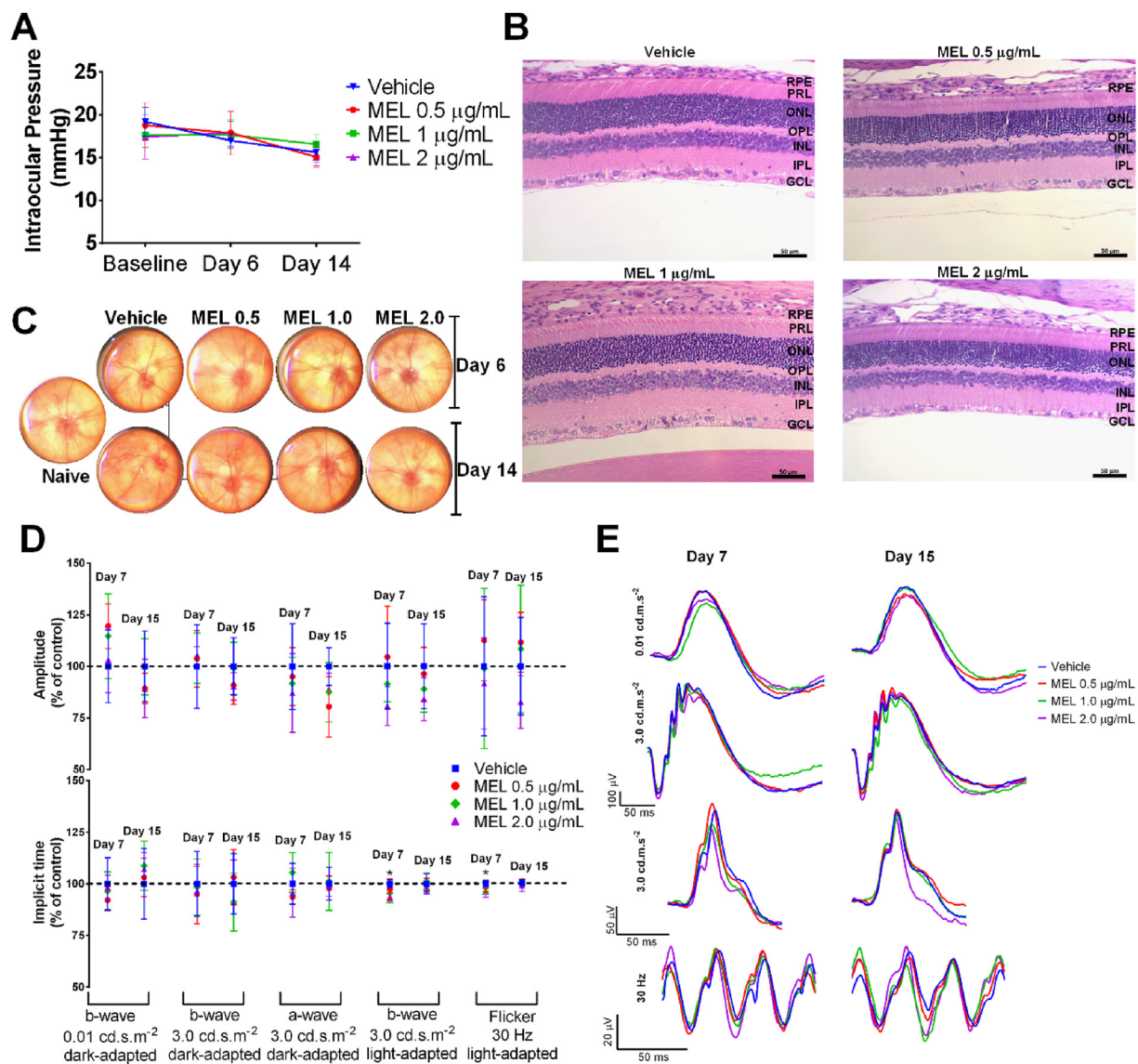

Fig. 3. Melittin 0.5, 1, and 2 μg/mL are safe for intravitreal administration. (A) The IOP of melittin-treated animals measured at baseline, 6 and 14 days after the intravitreal injections was not significantly different from the vehicle group at all time-points. (B) Eye fundus images representative of vehicle, naïve, and melittin-treated animals showing preserved retinal vasculature and optic nerve head, as well as the absence of vitreous opacity in all groups, after 6 and 14 days of the intravitreal injections. (C) Representative photomicrographs of eyes enucleated 15 days after the intravitreal injection of melittin 0.5, 1, and 2 μg/mL or vehicle, evidencing an organized retina with preserved morphology and with no signs of inflammation or degeneration. (D) ERG examinations recorded 7 and 15 days after intravitreal melittin or vehicle showing preserved dark- and light-adapted parameters, except for a transient shorter implicit-time in the light-adapted exam of animals treated with MEL 2 μg/mL. (E) Similar mean ERG curves were observed for all groups evaluated 7 and 15 days after treatment. Data are mean ± SD, n = 4/group; *p < 0.05 vs vehicle-treated animals; MEL: Melittin; GCL: ganglion cell layer; IPL: inner plexiform layer; INL: inner nuclear layer; OPL: outer plexiform layer; ONL: outer nuclear layer; PRL: photoreceptor layer; RPE: retinal pigment epithelium cells. Bar = 50 μm.

when compared to the vehicle group ($p < 0.05$ and $p < 0.01$ respectively). This alteration was regarded as transient, once there was no significant difference on the exam carried out 15 days after the injections. Altogether, these findings support the safety of MEL 0.5, 1, and 2 μg/mL for intravitreal administration.

3.4. MEL localization in the retina following intravitreal injection

Direct fluorescence microscopy was used to localize MEL conjugated with FITC in rats' retina 2 and 8 h after the intravitreal injection. Animals receiving intravitreal FITC solution and vehicle (saline) were used for qualitative comparison. At 2h post-injection, fluorescent signals were noticed in RPE and PRL of the retinas from animals receiving MEL-FITC (Fig. 4). The same was observed, although with lower intensity, in the FITC group, along with some fluorescent signals in the GCL. At 8h post-injection, however, no evident fluorescence was observed in the retinas of animals that received FITC solution, suggesting its elimination. Differently, after 8h, MEL-FITC injected animals still exhibited fluorescence in the PRL, with higher intensity when compared to the previous time-point. Also, some fluorescence signal was noticed in the GCL of MEL-FITC group at this time. These data indicate the presence of MEL in rats' retina for at least 8h after the injection and suggests that the peptide is able to reach the outer retina. The photomicrograph of the vehicle group confirms that background signals resulting from retinal autofluorescence were reduced prior to the other groups' analysis.

3.5. Melittin reduces blood vessels growth in the CAM model

The effect of MEL on blood vessels growth in the CAM was assessed by determining the relative vascularized area of the CAM, after treatment with MEL 0.5, 1, 2 μg/mL, bevacizumab (positive control), and saline (negative control). As expected, bevacizumab 5 mg/mL promoted a significant reduction of $40 \pm 9\%$ in the mean vascularized area (Fig. 5A) in comparison to the negative control treated with saline ($p < 0.0001$). Similarly, treatment with MEL 0.5, 1 and 2 μg/mL significantly reduced the mean vascularized area in $28 \pm 8\%$, $30 \pm 10\%$, and $37 \pm 12\%$, respectively, when compared to the negative control ($p < 0.0001$). There was no significant difference between bevacizumab and MEL 2 μg/mL ($p > 0.05$) groups. No signs of acute inflammation and vascular proliferation were observed on the CAM after treatment with MEL, as shown in the representative CAM images (Fig. 5B). Thus, these data confirm safety of MEL and suggest its antiangiogenic effect for all tested concentrations in the CAM model.

3.6. Melittin protects ARPE-19 cells from LPS-induced inflammatory response

The effect of pre-treatment with MEL on the inflammatory response induced by LPS in ARPE-19 cells was assessed by measuring levels of IL-6, IL-8, IL-1β, TNF-α, INF-γ, IL-17A, TGF-β1, and nitrite in the supernatant. Cells stimulated with LPS 10 μg/mL showed increased levels of IL-6, IL-8, and nitrite, when compared to control cells ($p = 0.0003$ for IL-8 and $p < 0.0001$ for IL-6 and nitrite) (Fig. 6). Levels of IL-1β, TNF-α, INF-γ, IL-17A, and TGF-β were below the minimum detectable concentration (MDC) in all groups evaluated (MDC = 2.15; 1.96; 1.79; 0.71; and 2.57 pg/mL, respectively). Although pre-treatment with MEL in all tested concentrations reduced the levels of IL-6, IL-8, and nitrite in LPS-activated cells, this decrease was not significant for nitrite and IL-8 levels in MEL 0.5 μg/mL treated cells ($p > 0.05$). However, IL-6 levels were significantly lower in all MEL treated groups when compared to untreated LPS-activated
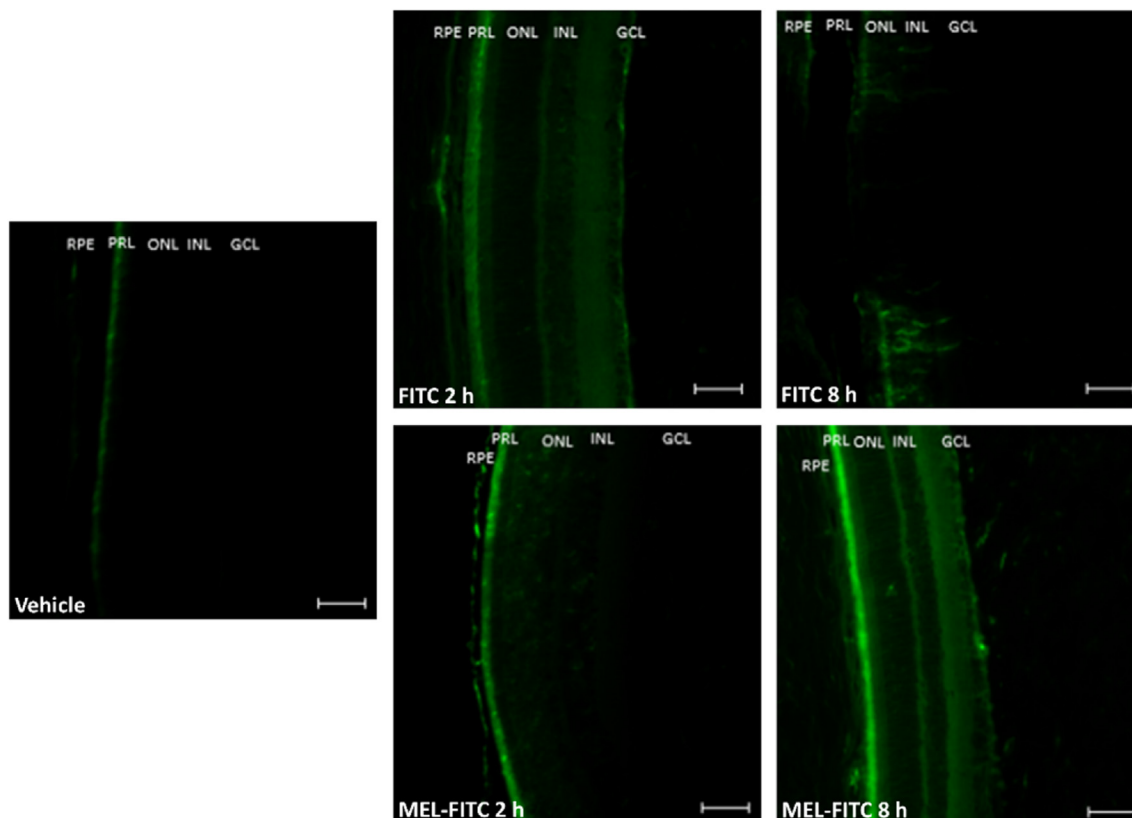

Fig. 4. Melittin conjugated with FITC penetrates through the retina and reaches the outer retina. Fluorescence photomicrographs representative of rats' retinas after 2 and 8h of intravitreal injection of melittin conjugated with FITC, FITC solution, or vehicle. MEL-FITC group showing fluorescent signals in the PRL and RPE after 2 and 8h, with additional signals in the GCL after 8h, while the FITC group exhibited fluorescence in PRL, RPE, and GCL after 2h with no evident signals after 8h; n = 2/group. MEL-FITC: melittin conjugated with FITC; FITC: fluorescein isothiocyanate; GCL: ganglion cell layer; INL: inner nuclear layer; ONL: outer nuclear layer; PRL: photoreceptor layer; RPE: retinal pigment epithelium cells. Bar = 50 μm.
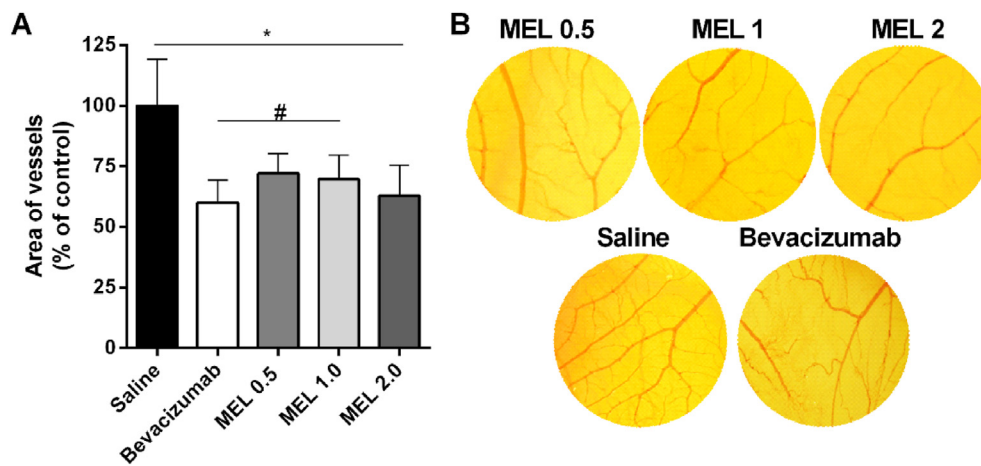
Fig. 5. Melittin inhibits angiogenesis in the chorioallantoic membrane. Chick embryos chorioallantoic membranes were treated with melittin 0.5, 1, and 2 μg/mL, bevacizumab 5 mg/mL, or saline on the 5th and 6th day after fertilization and photographed on the following day. (A) Melittin at all concentrations significantly reduced the vascularized area of the CAM in comparison to saline-treated group. (B) Representative photomicrographs of the CAM, taken 1 day after the last administration of each treatment. MEL: melittin. Data are mean ± SD, n = 12/group; *p < 0.05 vs saline group; #p < 0.05 vs bevacizumab.
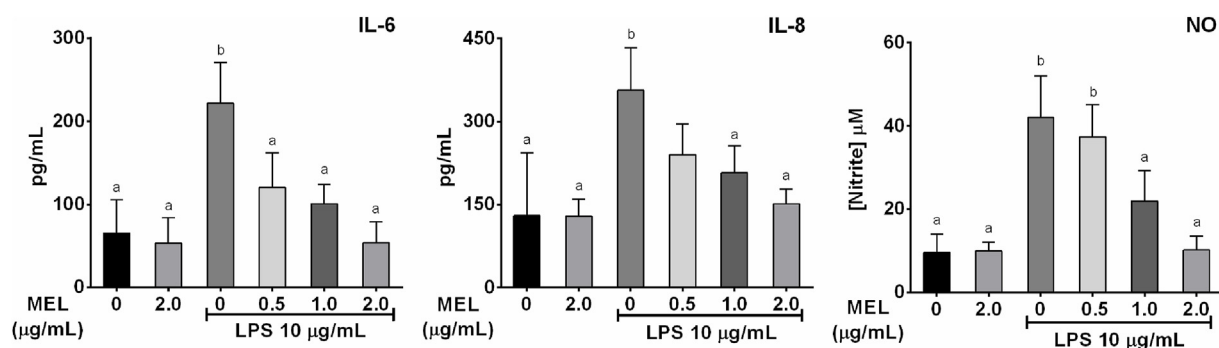

Fig. 6. Melittin reduces LPS-induced release of pro-inflammatory cytokines in ARPE-19 cells. Pre-treatment with melittin 1 and 2 μg/mL for 1h prior stimulation with LPS 10 μg/mL for 24h decreased IL-6, IL-8, and nitrite levels in the supernatant, determined by flow cytometry and Griess assay, respectively. Melittin 2 μg/mL did not stimulate de production of the proinflammatory markers measured in this assay in ARPE-19 cells. Data are mean ± SD, n = 4/group; [a] p < 0.05 vs untreated LPS-activated cells; [b] p < 0.05 vs control cells; MEL: melittin; LPS: lipopolysaccharide; NO: nitric oxide.

cells (p = 0.0027, p = 0.0003 and p < 0.0001 for MEL 0.5, 1 and 2 μg/mL, respectively). Likewise, pre-treatment with MEL 1 and 2 μg/mL resulted in significantly reduced levels of nitrite and IL-8 in comparison to untreated LPS-activated cells (IL-8: p = 0.0158 and p = 0.0005 for MEL 1 and 2 μg/mL respectively; nitrite: p = 0.0051 and p < 0.0001 for MEL 1 and 2 μg/mL respectively). Cells treated with MEL 2.0 μg/mL without LPS activation did not present any significant alteration in IL-6, IL-8, and nitrite levels when compared to control cells, that received only medium (p > 0.05). These results indicate the potential protective anti-inflammatory effect of MEL in ARPE-19 cells and support the following in vivo studies.

3.7. Intravitreal melittin alleviates ocular inflammation in rats

Rats with uveitis induced by BCG were treated with intravitreal MEL 0.5, 1.0, and 2.0 μg/mL, sterile saline (vehicle), or dexamethasone sodium phosphate (4 mg/mL), 3 days after disease induction. Clinical, morphological, and functional evaluation, in addition to immunological characterization, were conducted to assess the efficacy of intravitreal MEL for treatment of intraocular inflammation.

ERG examinations were performed at baseline, after uveitis induction, and 7 days following the IVT injections of MEL, to evaluate retinal function along the disease course and after treatments. As shown in Fig. 7A, there was no difference in a- and b-wave mean amplitudes recorded at baseline (p > 0.9999) for all groups evaluated. After disease induction, however, all animals receiving IVT injection of BCG presented significantly decreased a- and b-wave mean amplitudes in the maximum scotopic response when compared to healthy animals (p < 0.0001). Still, there was no significant difference among all groups with uveitis at this

time-point (p > 0.9999). Nevertheless, the exam recorded 7 days after IVT treatments revealed different responses for each group, as shown in more detail in Fig. 7B. Animals treated with MEL 1 and 2 μg/mL showed significantly improved amplitudes for both intensities evaluated in the light-adapted condition (Fig. 7B), in comparison to vehicle group (MEL 1 and 2 μg/mL respectively: p < 0.0001 and p = 0.0341 for b-wave at 0.01 cd.m.s^{-2}; p < 0.0001 and p = 0.0193 for b-wave at 3.0 cd.m.s^{-2}; p = 0.0039 and p = 0.0393 for a-wave at 3.0 cd.m.s^{-2}). The same was observed in rats treated with intravitreal dexamethasone (p = 0.0008 for b-wave at 0.01 cd.m.s^{-2}, p = 0.0192 and p = 0.0273 for a and b-wave at 3.0 cd.m.s^{-2}). Although animals treated with MEL 0.5 μg/mL showed improved mean amplitude, the values were not statistically different from the vehicle-treated group (p > 0.05). However, when comparing dexamethasone and all MEL-treated groups, there was no significant difference in the mean amplitude values (p > 0.05). The same result was reported in the dark-adapted exam, with dexamethasone, MEL 1 and 2 μg/mL promoting a significant improvement in b-wave and flicker peak (dexamethasone, MEL 1, and 2 μg/mL respectively: p = 0.0320, p = 0.0001, and p = 0.0214 for b-wave; p < 0.0001, p = 0.0120, and p = 0.0118 for flicker). No significant changes were detected in the implicit time in both light- and dark-adapted conditions (Fig. 7B). Mean ERG curves responses are shown in Fig. 7C, where it is noticeable the improvement after intravitreal treatment with MEL.

ERG data correlated with clinical and histopathological findings. Ophthalmic examination performed 2 days after IVT injections of BCG, detected inflammatory signs involving the anterior and posterior segment of the eyes. A mean score relative to ciliary injection of 2.3 ± 0.2+/4+, iris congestion of 2.2 ± 0.2+/4+, and conjunctival hyperemia of 1.9 ± 0.2+/4+ was observed. An intense vitreous haze was also
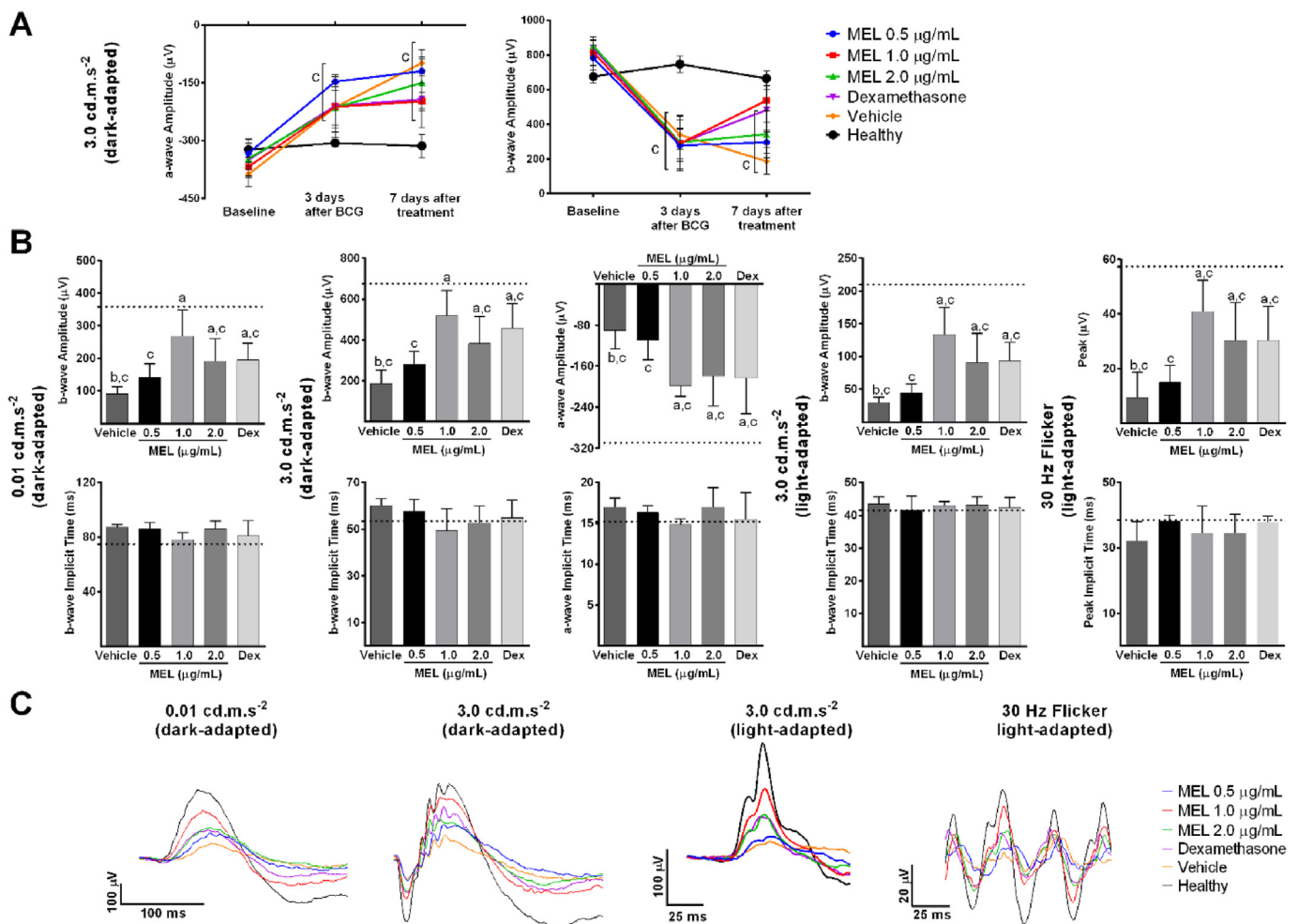
Fig. 7. Intravitreal melittin improves retinal function in rats with BCG-induced uveitis. Rats inoculated with two weekly doses of BCG received 7 days later an intravitreal injection of the same antigen and were treated with intravitreal melittin 0.5, 1, or 2 μg/mL, dexamethasone, or saline. (A) ERG examinations performed at baseline, 3 days after BCG intravitreal injection, and 7 days after treatment showed a significantly reduced retinal function after disease induction for all groups with uveitis when compared to healthy animals and different responses after each treatment. (B) Rats treated with MEL showed significantly higher a and b-wave amplitudes compared to vehicle-treated group, with values similar to dexamethasone-treated animals, in light- and dark-adapted exams. (C) Mean ERG curves showing improved responses with treatment with MEL and dexamethasone. Data are mean ± SD, n = 4/group. [a] $p < 0.05$ vs vehicle; [b] $p < 0.05$ vs dexamethasone; [c] $p < 0.05$ vs healthy group. Dashed lines represent mean values from the healthy group. MEL: melittin; DEX: dexamethasone.

detected, with a mean score of 3.6 ± 0.4+/4+. The inflammatory response was consistent in all groups with uveitis and healthy animals presented no abnormalities. Animals were examined once again 6 days after treatment, and representative images of slit-lamp biomicroscopy are shown in Fig. 8. Animals treated with vehicle (saline) presented mild to moderate (1–2+/4+) iris congestion, as well as the presence of cells in the anterior chamber (1–2+/4+), and fibrin deposits on the lens capsule. Posterior subcapsular cataract of 2+/4+ and severe vitreous haze (4+/4+) were also observed. Animals treated with MEL 0.5 μg/mL showed apparent normal conjunctiva. Yet, mild iris congestion (0–1+/4+) and anterior chamber cells (0–1+/4+) were detected, in addition to fibrin deposition on the lens capsule, posterior subcapsular cataract (1+/4+), and vitreous haze (3–4+/4+). Treatment with MEL 1 μg/mL resulted in an improvement of the inflammatory reaction in the anterior chamber, which presented an apparent normal aspect. Still, iris congestion of 0–1+/4+ was identified, along with fibrin deposits on the lens capsule and vitreous haze (2–3+/4+). The same findings were identified in animals treated with MEL 2 μg/mL, with a slight improvement in vitreous haze (1–2+/4+). Similarly, animals treated with dexamethasone 4 mg/mL presented anterior chamber and conjunctiva with normal aspect. Mild iris congestion (0–1+/4+) and marked vitreous haze (3+/4+) were also detected in this group. No clinical alterations were identified in healthy animals.

These findings suggest a clinical improvement after treatment with IVT MEL and with dexamethasone.

This result was confirmed in the histopathological analysis of the eyes enucleated 7 days after treatment (Fig. 9). The photomicrographs showed that animals treated with vehicle (saline) exhibited an intense inflammatory reaction involving the uveal tract. Inflammatory cells were seen infiltrating the vitreous and the retina, whose structure was disorganized and presenting abnormal folds. The photoreceptor layer was disrupted and damage was also observed in the ganglion cell layer of this group. The inflammatory response was less intense in animals treated with MEL 0.5 μg/mL, although inflammatory cells in the ciliary body and vitreo-retinal interface were still found. The retina was slightly more organized but folds were still detected. The inflammatory response was attenuated in animals treated with MEL 1 μg/mL, MEL 2 μg/mL, and DEX. These groups exhibited a more preserved retinal structure and mild inflammatory infiltrate in the ciliary body and retina. No histopathological changes were observed in eyes healthy animals.

In order to characterize the inflammatory infiltrate and assess levels of pro-inflammatory markers in the posterior segment after treatment with MEL, activity of MPO and NAG in these tissues was determined, as well as concentration of IL-6, IL-1β, TNF-α, and CXCL-1. Animals treated with vehicle showed significantly higher activity of NAG ($p < 0.0001$)
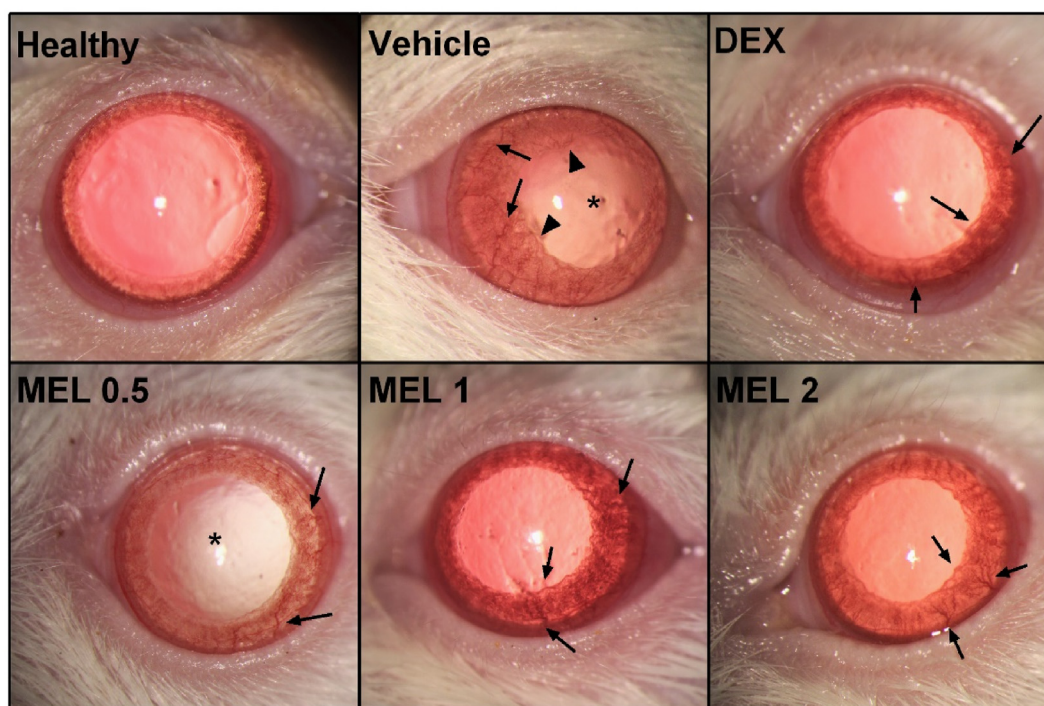
Fig. 8. Intravitreal melittin ameliorates clinical manifestation of uveitis in rats. Representative images were obtained with a slit-lamp, 6 days after intravitreal treatment with melittin, dexamethasone, or saline in rats with BCG-induced uveitis. Clinical signs of ocular inflammation, including iris congestion (arrows), posterior subcapsular cataract (asterisks), and synechiae (arrowheads) were observed in saline-treated animals. MEL 0.5 improved conjunctival hyperemia, although mild iris congestion and posterior subcapsular cataract were still present. An attenuated inflammatory reaction was observed in animals treated with MEL 1, 2 μg/mL and dexamethasone, whose anterior segment presented a normal aspect, except for mild iris congestion. Healthy animals exhibited eyes with a normal aspect; n = 6 per group.

and MPO (p = 0.0038) when compared to the healthy group, as depicted in Fig. 10. Treatment with MEL 0.5 μg/mL was able to significantly reduce the activity of NAG (p = 0.0157), but not of MPO (p > 0.05) when compared to vehicle-treated animals. MEL 0.5 also promoted a significant reduction in IL-6 (p = 0.0038) and nitrite (p = 0.0018) levels (Fig. 10), whereas CXCL-1 and IL-1β levels did not differ from the vehicle group (p > 0.05). Rats treated with intravitreal MEL 1 μg/mL, MEL 2 μg/mL and DEX showed decreased activities of NAG and MPO in comparison to the vehicle group (NAG: p = 0.0035; p = 0.0240; p = 0.0008; MPO: p = 0.0089; p = 0.0384; p = 0.0131 for MEL 1, MEL 2 and DEX respectively). This effect was accompanied by significantly reduced levels of nitrite, IL-6, IL-1β, TNF-α, and CXCL-1 in posterior segment tissues (nitrite: p = 0.0018, p = 0.0071, and p = 0.0103 for MEL 1, MEL 2 and DEX respectively; IL-1β: p = 0.0004, p = 0.0005, and p < 0.0001; TNF-α: p = 0.0340, p = 0.0260, and p = 0.0022; CXCL-1: p = 0.0013, p = 0001, and p < 0.0001; IL-6: p < 0.0001. There was no significant difference between MEL 1, MEL 2, and DEX groups in all analyses performed. The same was observed when comparing MEL 1, MEL 2, and healthy animals regarding IL-6, IL-1β, MPO, and NAG levels (p > 0.05).

4. Discussion

This study demonstrates the potential of intravitreal MEL for ocular therapy, particularly for management of inflammation and neovascularization. These results were confirmed in vitro, using retinal cells, and in vivo using chick embryo chorioallantoic membranes and rats. Treatment of noninfectious uveitis can be challenging to clinicians due to its complex pathogenesis and diverse etiology, in addition to potentially severe adverse events associated with the mainstay therapy (Hou et al., 2020). MEL is the major component of bee venom and has shown therapeutic effects in different models of inflammatory diseases, although not yet explored in an intraocular setting (Lee et al., 2014; Lee and Bae, 2016;

Kim et al., 2017; Lin et al., 2017). Here, we report the safety of MEL for intravitreal administration and its ability to alleviate clinical, morphological, and functional ocular changes observed in a model of uveitis induced by BCG in rats.

MEL at low concentrations did not affect the viability of ARPE-19 cells as well as did not cause vascular damage to the CAM and was safe for intravitreal administration in rats. MEL at concentrations of 1.5 μg/mL and lower did not reduce ARPE-19 cells viability after 24 and 48h of exposure. In contrast, only concentrations higher than 3.0 μg/mL significantly affected cells viability after 72h of treatment. Srivastava et al. (2018) observed a similar behavior in ARPE-19 cells and suggested that since the substance induced only 40–50% mortality at 24h, surviving cells could have had sufficient growth to achieve higher viabilities at 72h, which is consistent with the population doubling time reported for ARPE-19 cells (Heimsath et al., 2006; Liang et al., 2010; Liu et al., 2017). Also, the cytotoxic effect of MEL is associated with its interaction with cell membranes, which can lead to its membrane-disrupting activity (Liu et al., 2016; Sabapathy et al., 2020). This interaction has been reported as rapid and dependent on several elements, such as peptide/lipid ratio and peptide concentration, although not described as time-dependent (Jamasbi et al., 2016; Hong et al., 2019; Pereira et al., 2020). Altogether, these factors might have contributed to the difference observed in long exposure times, an outcome also reported in other cell viability studies with MEL (Park et al., 2011; Tipgomut et al., 2018; Yang et al., 2022).

HET-CAM is an alternative eye irritation assay that uses the vascularized chorioallantoic membrane of fertilized chicken eggs. The CAM presents similarities to the retina and to mucosal tissues of the human eye, representing a suitable model to predict ocular toxicity after exposure to a tested compound (Leng et al., 2004; Hao et al., 2014). The absence of vascular reactions after administration of MEL at concentrations further chosen for the in vivo study is crucial to corroborate this
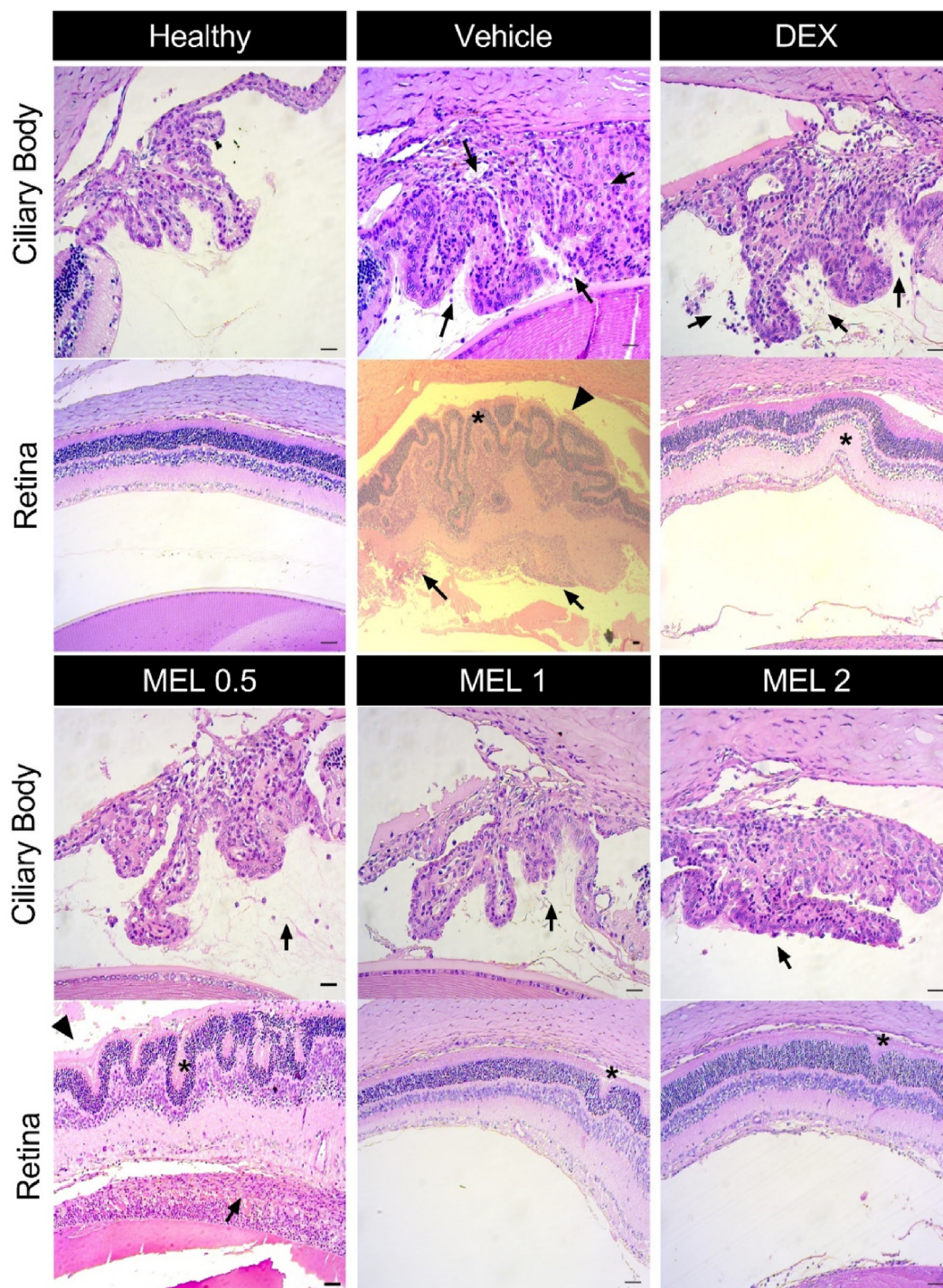
Fig. 9. Intravitreal melittin attenuates morphological changes in rats with uveitis. Representative H&E photomicrographs of eyes enucleated 7 days after intravitreal treatment with melittin, dexamethasone, or saline in rats with BCG-induced uveitis. Severe retinal folds (asterisks) and disorganized retinal structure were observed in the saline-treated group, in addition to damaged photoreceptors layer (arrowhead) and inflammatory infiltrate (arrows) involving the ciliary body region and vitreous cavity. MEL 0.5-treated group showed a less intense inflammatory response in the ciliary body region, the retina slightly more organized but with an intense inflammatory infiltrate. Treatment with MEL 1, 2, and DEX attenuated the ocular inflammatory reaction, with animals exhibiting improved retinal structure and mild inflammatory infiltrate in the ciliary body region. No abnormal histological findings were observed on healthy animals; n = 3 per group.

choice since hemolysis is a toxic reaction previously reported with MEL (Rady et al., 2017). Somwongin et al. (2018) reported a vascular response in a HET-CAM assay with MEL, but at concentrations 1000x higher than the ones evaluated in this work. At the evaluated concentrations of this study, MEL did not cause vascular damage or any other signal of toxicity to the CAM.

When evaluating ocular toxicity of new drug candidates, it is important to conduct electrophysiological, clinical and histopathological studies, as here performed (Onodera et al., 2015; Shibuya et al., 2015). ERG examinations provide information regarding particular retinal cells and their function, being widely applied to assess toxicity of new ocular therapies (Huang et al., 2015; Paiva et al., 2021; Toledo et al., 2019).
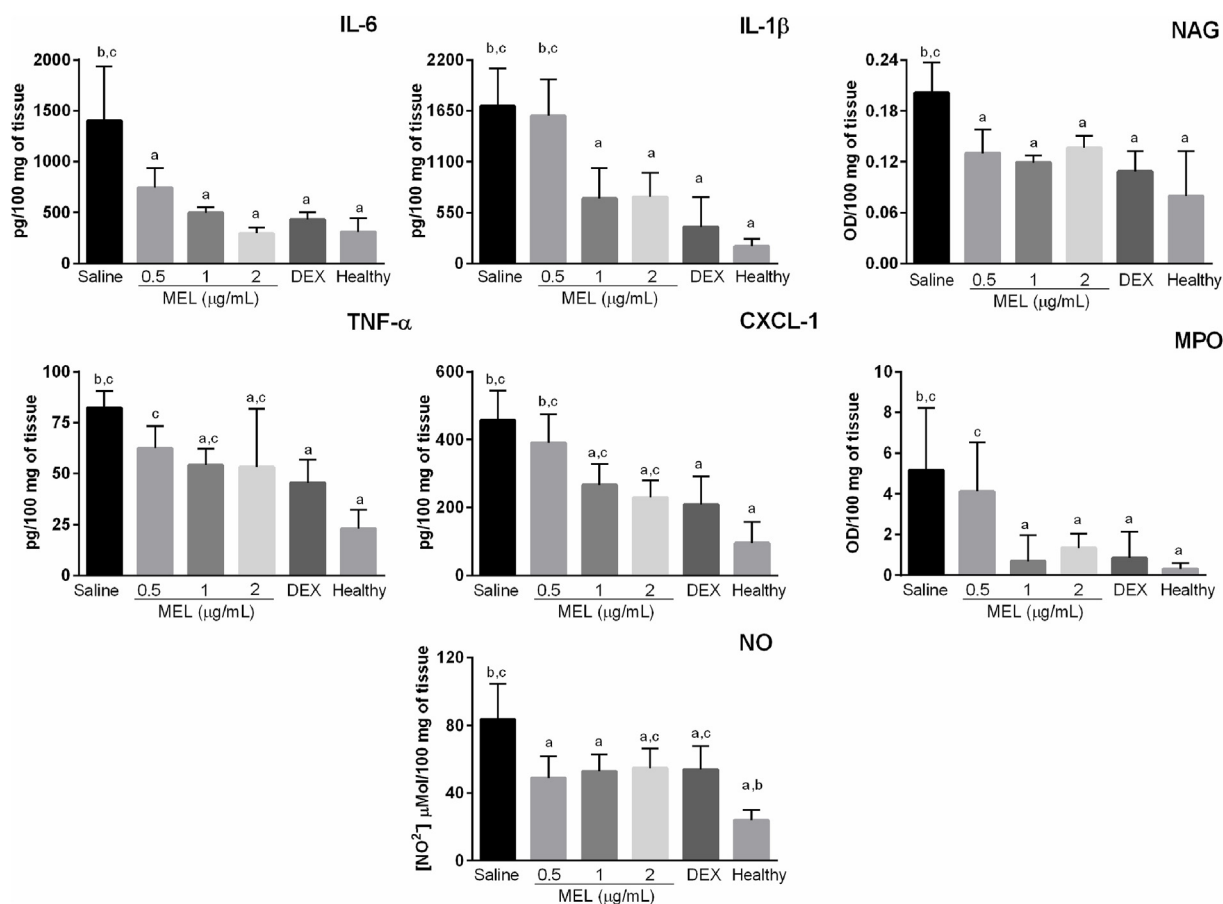
Fig. 10. Treatment with intravitreal melittin decreases levels of pro-inflammatory markers in the posterior segment of rats with uveitis. Eyes were enucleated 7 days after treatment with melittin, dexamethasone, or saline, and cytokines/chemokine levels were determined by ELISA while nitrite concentration was assessed by the Griess reagent assay and NAG and MPO activity by a colorimetric reaction. Treatment with DEX, MEL 1 and 2 µg/mL was able to decrease the levels of all markers in comparison to the vehicle-treated group, whereas MEL 0.5 did not significantly affect CXCL-1, TNF-α, and MPO levels. Data are mean ± SD, n = 4/group. [a] $p < 0.05$ vs vehicle; [b] $p < 0.05$ vs dexamethasone; [c] $p < 0.05$ vs healthy group. MEL: melittin; DEX: dexamethasone; MPO: myeloperoxidase; NAG: N-acetylglucosaminidase; NO: nitric oxide.

Once elements of a- and b-waves were not affected in both scotopic and photopic conditions, the functionality of rods (a-wave, scotopic) and rod-driven On-bipolar cells (b-wave, scotopic) were preserved, as well as the activity of cones on bipolar cells (photopic) and the photo-transduction kinetics (implicit-times) (Robson et al., 2018; Mcclinton et al., 2019). Clinical and histopathological evaluations complemented the ERG results, all confirming the safety of intravitreal MEL. Altogether, these results indicate that MEL does not cause any damage to intraocular tissues and support its application on animal models of ocular diseases. Additionally, intravitreal MEL conjugated with FITC was detected in the inner and outer retina, suggesting the ability of this peptide to penetrate through the retina and reach cells highly affected during an inflammatory process (Nguyen and Rao, 2011; Taylor et al., 2021). These qualitative data are important when targeting retinal cells through intravitreal injections, once several biological barriers, including the vitreous, inner limiting membrane, and extracellular matrix, must be overcome to reach these cells (Huang and Chau, 2019).

The concentrations of MEL safe for intravitreal administration also showed in vivo antiangiogenic activity in the CAM assay. This effect was similar to the positive control, bevacizumab, which is an anti-vascular endothelial growth factor (VEFG) monoclonal antibody highly applied in clinical practice to treat ocular neovascularization (Formica et al., 2021). Other studies have explored the antiangiogenic activity of MEL, especially for cancer treatment (Liu et al., 2016; Rady et al., 2017). Zhang et al. (2016) showed the ability of MEL to inhibit capillary tube formation

in human umbilical vein endothelial cells (HUVEC) transfected with cathepsin-S and its suppressing effect on the expression of components of VEGF-A/VEGFR-2/MEK1/ERK1/2 signaling pathway in hepatocellular carcinoma cells. Likewise, El Bakary et al. (2020) reported a decreased expression of VEGFR-2, COX-2, and prostaglandin E2 in VEGF-A transfected HUVECs treated with MEL, along with reduced ERK1/2 and JNK phosphorylation and increased p38 phosphorylation. In the eye, pathological angiogenesis can lead to significant visual loss, especially when affecting the retina and choroid (Cabral et al., 2017). VEGF is a key regulator of ocular angiogenesis, being an important target in several conditions, including diabetic retinopathy, neovascular age-related macular degeneration, retinopathy of prematurity, retinal vein occlusions, uveitis, and neovascular glaucoma (Usui et al., 2015; Cabral et al., 2017). Although current anti-VEGF therapies have shown to be effective for the treatment of most eye diseases related to neovascularization, there are still some concerns regarding resistance and off-target effects, which stimulate the investigation of new therapeutic strategies (Usui et al., 2015). Thus, the suggested antiangiogenic effect of MEL at safe concentrations for intravitreal administration is promising, although more studies are needed to ascertain its mechanism of action in an ocular model of neovascularization and to screen for off-target effects.

MEL also showed a protective effect from the inflammatory response induced by LPS in ARPE-19 cells. Activation with LPS in retinal cells has been widely used to evaluate new therapies for ocular inflammation (Maugeri et al., 2018; Ozal et al., 2018; Zhang et al., 2018; Girol et al.,

2019). ARPE-19 cells constitutively express toll-like receptor 4 (TLR4), which in conjunction with CD14 and MD-2 (myeloid differentiation protein-2), co-receptors also expressed in these cells, mediates LPS recognition (Chui et al., 2009; Mai et al., 2014). The formation of this complex leads to the production of proinflammatory mediators potentially involved in retinal degeneration and ocular inflammation (Elner et al., 2005; Chui et al., 2009). In this work, this was observed by the increased levels of IL-6, IL-8, and nitrite in the supernatant of LPS-activated cells. In the RPE, IL-6 is involved in acute inflammation while IL-8 is a granulocyte-attracting chemokine, with both having functional importance in angiogenesis and LPS-induced toxicity (Arjamaa et al., 2017). During inflammation, iNOS catalyzes the formation of NO, which is rapidly metabolized into nitrite and nitrate, the mediators of its toxicity (Arroul-lammali et al., 2012). Cells pre-treated with MEL presented lower levels of these mediators, comparable to controls, suggesting a protective effect (Taylor et al., 2021). A similar outcome reported by Moon et al. (2007) in microglial cells was associated with effects of MEL in downregulation of NF-κB activation, and inhibition of JNK and protein kinase B (Akt) pathways. Park et al. (2007) also observed a decrease in nitrite levels in the supernatant of cells stimulated with LPS in the presence of MEL. The authors attributed this result to the high binding affinity of MEL and IKK which consequently suppresses LPS-induced IKKβ activity, NF-κB signaling, and the expression of COX-2 and iNOS. Other studies have reported the activation of the NF-κB and MAPKs signaling pathways as a result of LPS stimulation in ARPE-19 cells, with following increase in NO, IL-6, and IL-8 levels (Jung et al., 2014; Girol et al., 2019; Song et al., 2020). Overall, it suggests that the observed effect of MEL on ARPE-19 cells could be related to its activity on NF-κB and MAPKs signaling pathways, as reported in other cell lines (Moon et al., 2007; Lee and Bae, 2016). Yet, the exact anti-inflammatory mechanism of MEL on RPE cells still has to be elucidated.

The effect of intravitreal MEL was assessed in an experimental model of BCG-induced panuveitis in rats. The ocular manifestations of uveitis observed in this work are consistent with other studies using the same experimental model (Castro et al., 2020; Toledo et al., 2021). Treatment with MEL was able to alleviate clinical signs of intraocular inflammation, showing a response similar to that of animals treated with dexamethasone. The preservation/restoration of retinal structure and function in MEL-treated groups was confirmed in histopathological and ERG analysis. ERG examinations can be a useful clinical tool in uveitis, allowing the monitoring of the disease severity and progression, along with the therapy response (Chen et al., 2013; Moschos et al., 2014). ERG changes in uveitis may result from photoreceptor damage, which occurs due to the presence of inflammatory infiltrate in the posterior segment (Paiva et al., 2021). In fact, disruption of blood-ocular barriers characterizes experimental models of ocular inflammation and leads to infiltration of inflammatory cells, including macrophages and polymorphonuclear leukocytes (Bousquet et al., 2015). In this work, this process is indicated by the increased activity of NAG and MPO, which was significantly higher in the vehicle-treated group compared to all the others. NAG is produced mainly by macrophages, indicating their accumulation and activation, whereas MPO is secreted during neutrophil activation/degranulation (de Souza et al., 2012; Arafat et al., 2014). Chu et al. (2016) observed higher MPO activity following an increase in inflammatory cells in ocular tissues during inflammation, possibly reflecting neutrophil activation. Recruitment of inflammatory cells from the circulation to the eye also involves release of proinflammatory cytokines and chemokines (Diedrichs-Möhring et al., 2018). Indeed, higher levels of IL-6, IL-1β, TNF-α, CXCL1, and nitrite were detected in all groups with uveitis in this study. Increased production and secretion of these mediators have also been observed in ocular fluids and serum from patients with uveitis when compared to healthy controls (Carreño et al., 2016; Fukunaga et al., 2020). Furthermore, TNF-α, IL-6, and IL-1β are central mediators of ocular inflammation, which lead to activation of both innate and adaptive immunity (Reddy et al., 2018). In addition, increased production of NO during the inflammatory process within the eye can result in cell damage, especially photoreceptors, which was detected in the histopathological analysis of the vehicle-treated group (Saraswathy and Rao, 2008). The therapeutic effect of MEL in inflammation has been demonstrated in different animal models including acute liver failure, renal fibrosis, acne, atopic dermatitis, and chronic prostatitis (Park et al., 2012; Lee et al., 2014; An et al., 2016; Kim et al., 2017; Lin et al., 2017). This outcome was mainly associated with the regulation of the NF-κB signaling pathway by MEL, which, in fact, has been proposed as its anti-inflammatory mechanism (Son et al., 2007; Lee et al., 2014; Lee and Bae, 2016). In this regard, Son et al. (2007) suggested that MEL modifies the activities of IKKα and IKKβ and inhibits the release of IκBα and IκBβ. This likely happens due to an interaction between MEL and the sulfhydryl group of IKKα and IKKβ, which results in NF-κB inactivation and consequent reduction in inflammatory mediators' production. The authors also mentioned that MEL can interact directly with p50 of NF-κB, inhibiting its translocation into the nucleus. Still, further investigations are needed to evaluate whether the anti-inflammatory effect of MEL observed in the experimental model of uveitis used in our study is associated with regulation of this pathway.

5. Conclusion

This study shows for the first-time evidence that MEL may be a potential candidate for treatment of eye diseases involving angiogenesis and inflammation. Once clinical application of melittin is limited due to its potential toxicity, we provided a range of concentrations suitable and safe for intravitreal administration, as demonstrated in vitro and in vivo through different assays. Therefore, it allows further exploration of this peptide in different ocular disorders, in addition to stimulating the study of MEL derivatives and delivery systems containing melittin in ophthalmology. Future studies are expected to provide a more in-depth pharmacological evaluation of pathways affected by MEL in the context of ocular inflammation and angiogenesis.

CRediT authorship contribution statement

Brenda Fernanda Moreira Castro: Conceptualization, Methodology, Investigation, Formal analysis, Writing – original draft. **Carolina Nunes da Silva:** Investigation, Validation, Writing – review & editing. **Lídia Pereira Barbosa Cordeiro:** Investigation, Methodology, Writing – review & editing. **Sarah Pereira de Freitas Cenachi:** Investigation, Methodology, Writing – review & editing. **Daniel Vitor Vasconcelos-Santos:** Investigation, Methodology, Writing – review & editing. **Renes Resende Machado:** Conceptualization, Validation, Resources, Writing – review & editing. **Luiz Guilherme Dias Heneine:** Investigation, Methodology, Writing – review & editing. **Luciana Maria Silva:** Resources, Methodology, Writing – review & editing. **Armando Silva-Cunha:** Conceptualization, Funding acquisition, Project administration, Writing – review & editing. **Silvia Ligório Fialho:** Conceptualization, Funding acquisition, Project administration, Writing – review & editing.

References

Ahmed, C.M., Ildefonso, C.J., Johnson, H.M., Lewin, A.S., 2020. A C-terminal peptide from type I interferon protects the retina in a mouse model of autoimmune uveitis. PLoS One 15 (2), 1–20. https://doi.org/10.1371/journal.pone.0227524.

An, H., Kim, J., Kim, W., Han, S., Park, K., 2016. The protective effect of melittin on renal fibrosis in an animal model of unilateral ureteral obstruction. Molecules 21 (1137). https://doi.org/10.3390/molecules21091137.

An, H., Kim, J., Kim, W., Gwon, M., Gu, H.M., Jeon, M.J., et al., 2018. Therapeutic effects of bee venom and its major component, melittin, on atopic dermatitis in vivo and in vitro. Br. J. Pharmacol. 175, 4310–4324. https://doi.org/10.1111/bph.14487.

Arafat, S.N., Suelves, A.M., Spurr-Michaud, S., James, C., Foster, S., Claes, H.D., et al., 2014. Neutrophil collagenase, gelatinase and myeloperoxidase in tears of Stevens-Johnson syndrome and ocular cicatricial pemphigoid patients. Ophthalmology 121 (1), 79–87. https://doi.org/10.1016/j.ophtha.2013.06.049.Neutrophil.

Arjamaa, O., Aaltonen, V., Piippo, N., Csont, T., Petrovski, G., 2017. Hypoxia and inflammation in the release of VEGF and interleukins from human retinal pigment epithelial cells. Graefe's Arch. Clin. Exp. Ophthalmol. https://doi.org/10.1007/s00417-017-3711-0, 0–5.

Arroul-lammali, A., Djeraba, Z., Belkhelfa, M., Belguendouz, H., Hartani, D., Lahlou-boukoffa, O.S., et al., 2012. Early involvement of nitric oxide in mechanisms of pathogenesis of experimental autoimmune uveitis induced by interphotoreceptor retinoid-binding protein (IRBP). J. Fr. Ophtalmol. 35 (4), 251–259. https://doi.org/10.1016/j.jfo.2011.05.003.

Aufschnaiter, A., Kohler, V., Khalifa, S., El-Wahed, A., Du, M., El-Seedi, H., et al., 2020. Apitoxin and its components against cancer, neurodegeneration and rheumatoid arthritis: limitations and possibilities. Toxins 12 (2), 66.

Banks, B.E.C., Dempsey, C.E., Pearce, F.L., Vernon, C.A., Wholley, T.E., 1981. New methods of isolating bee venom peptides. Anal. Biochem. 116 (1), 48–52. https://doi.org/10.1016/0003-2697(81)90320-1.

Bousquet, E., Zhao, M., Thillaye-goldenberg, B., Lorena, V., Castaneda, B., Naud, M.C., et al., 2015. Choroidal mast cells in retinal pathology A potential target for intervention. Am. J. Pathol. 185 (8), 2083–2095. https://doi.org/10.1016/j.ajpath.2015.04.002.

Cabral, T., Mello, L.G.M., Lima, L.H., Polido, J., Regatieri, C.V., Belfort Jr., R., et al., 2017. Retinal and choroidal angiogenesis: a review of new targets. Int. J. Retin. Vitr. 1–13. https://doi.org/10.1186/s40942-017-0084-9.

Carreño, E., Portero, A., Herreras, J., García-Vázquez, C., Whitcup, S., Stern, M., et al., 2016. Cytokine and chemokine tear levels in patients with uveitis. Acta Ophthalmol. 95 (5), 1–10. https://doi.org/10.1111/aos.13292.

Caspi, R.R., 2010. A look at autoimmunity and inflammation in the eye. J. Clin. Invest. 120 (9), 3073–3083. https://doi.org/10.1172/JCI42440.

Castro, B., Vieira, L., Vasconcelos-santos, D.V., Pereira, S., Cenachi, D.F., Araújo, O., et al., 2020. International Immunopharmacology Intravitreal thalidomide ameliorates inflammation in a model of experimental uveitis induced by BCG. Int. Immunopharm. 81 (November 2019), 106129. https://doi.org/10.1016/j.intimp.2019.106129.

Chen, J., Qian, H., Horai, R., Chan, C., Caspi, R.R., 2013. Use of optical coherence tomography and electroretinography to evaluate retinal pathology in a mouse model of autoimmune uveitis. PLoS One 8 (5). https://doi.org/10.1371/journal.pone.0063904.

Chen, C.L., Chen, J.T., Liang, C.M., Tai, M.C., Lu, D.W., 2017. Chen YH Silibinin treatment prevents endotoxin-induced uveitis in rats in vivo and in vitro. PLoS One 12 (4), 1–18. https://doi.org/10.1371/journal.pone.0174971.

Chu, C.J., Gardner, P.J., Copland, D.A., Liyanage, S.E., Gonzalez-Cordero, A., kleine Holthaus, S.-M., et al., 2016. Multimodal analysis of ocular inflammation using the endotoxin-induced uveitis mouse model. Dis. Model. Mech. 9 (4), 473–481. https://doi.org/10.1242/dmm.022475.

Chui, Jeanie J Y, Li, M.W.M., Girolamo, N.D., Chang, J.H., Mccluskey, P.J., Wakefield, D., 2009. Iris pigment epithelial cells express a functional lipopolysaccharide receptor complex. Immunol. microbiol. 51 (5), 2558–2567. https://doi.org/10.1167/iovs.09-3923.

da Silva, C.N., Dourado, L.F.N., de Lima, M.E., da Silva Cunha, A., 2020. Pnpp-19 peptide as a novel drug candidate for topical glaucoma therapy through nitric oxide release. Transl. Vis. Sci. Technol. 9 (8), 1–13. https://doi.org/10.1167/TVST.9.8.33.

de Smet, M.D., Taylor, S.R.J., Bodaghi, B., Miserocchi, E., Murray, P.I., Pleyer, U., et al., 2011. Understanding uveitis: the impact of research on visual outcomes. Prog. Retin. Eye Res. 30 (6), 452–470. https://doi.org/10.1016/j.preteyeres.2011.06.005.

de Souza, C.M., de Carvalho, L.F., Vieira, T. da S., Araújo e Silva, A.C., Lopes, M.T.P., Ferreira, M.A.N.D., et al., 2012. Thalidomide attenuates mammary cancer associated-inflammation, angiogenesis and tumor growth in mice. Biomed. Pharmacother. 66 (7), 491–498. https://doi.org/10.1016/j.biopha.2012.04.005.

Diedrichs-Möhring, M., Kaufmann, U., Wildner, G., 2018. The immunopathogenesis of chronic and relapsing autoimmune uveitis – lessons from experimental rat models. Prog. Retin. Eye Res. 65, 107–126. https://doi.org/10.1016/j.preteyeres.2018.02.003.

El Bakary, N.M., Alsharkawy, A.Z., Shouaib, Z.A., Barakat, E.M.S., 2020. Role of bee venom and melittin on restraining angiogenesis and metastasis in γ -irradiated solid ehrlich carcinoma- bearing mice. Integr. Cancer Ther. 19, 1–13. https://doi.org/10.1177/1534735420944476.

Elner, S.G., Petty, H.R., Elner, V.M., Yoshida, A., Bian, Z., Yang, D., et al., 2005. TLR4 mediates human retinal pigment epithelial endotoxin binding and cytokine expression AND. Invest. Ophthalmol. Vis. Sci. 46 (12), 2–8. https://doi.org/10.1167/iovs.05-0658.

Formica, M.L., Alfonso, H.G.A., Palma, S.D., 2021. Biological drug therapy for ocular angiogenesis: anti-VEGF agents and novel strategies based on nanotechnology. Pharmacol. Res. Perspect. 9 (2), 1–18. https://doi.org/10.1002/prp2.723.

Foster, C.S., Kothari, S., Anesi, S.D., Vitale, A.T., Chu, D., Metzinger, J.L., et al., 2016. The Ocular Immunology and Uveitis Foundation preferred practice patterns of uveitis management. Surv. Ophthalmol. 61 (1), 1–17. https://doi.org/10.1016/j.survophthal.2015.07.001.

Fukunaga, H., Kaburaki, T., Shirahama, S., Tanaka, R., Murata, H., Sato, T., et al., 2020. Analysis of inflammatory mediators in the vitreous humor of eyes with pan-uveitis according to aetiological classification. Sci. Rep. 10 (1), 1–12. https://doi.org/10.1038/s41598-020-59666-0.

Gamalero, L., Simonini, G., Ferrara, G., Polizzi, S., Giani, T., Cimaz, R., 2019. Evidence-based treatment for uveitis. Isr. Med. Assoc. 21, 3–7.

Girol, A.P., Mimura, K.K.O., Drewes, C.C., Bolonheis, S.M., Solito, E., Farsky, S.H.P., et al., 2019. Anti-inflammatory mechanisms of the annexin A1 protein and its mimetic peptide Ac2-26 in models of ocular inflammation in vivo and in vitro. J. Immunol. 190 (11), 5689–5701. https://doi.org/10.4049/jimmunol.1202030.

Haghi, G., Hatami, A., Mehran, M., 2013. Qualitative and quantitative evaluation of melittin in honeybee venom and drug products containing honey-bee venom. J. Apicult. Sci. 57 (2), 37–44. https://doi.org/10.2478/jas-2013-0015.

Hao, J., Wang, X., Bi, Y., Teng, Y., Wang, J., Li, F., et al., 2014. Fabrication of a composite system combining solid lipid nanoparticles and thermosensitive hydrogel for challenging ophthalmic drug delivery. Colloids Surf. B Biointerfaces 114, 111–120. https://doi.org/10.1016/j.colsurfb.2013.09.059.

Hassan, M., Karkhur, S., Bae, J.H., Halim, M.S., Ormaechea, M.S., Onghanseng, N., et al., 2019. New therapies in development for the management of non-infectious uveitis: a review. Clin. Exp. Ophthalmol. 47 (3), 396–417. https://doi.org/10.1111/ceo.13511.

Heimsath, E.G., Unda, R., Vidro, E., Muniz, A., Villazana-espinoza, E.T., Tsin, A., 2006. ARPE-19 growth and cell functions in euglycemic culture media. Curr. Eye Res. 31, 1073–1080. https://doi.org/10.1080/02713680601052320.

Hong, J., Lu, X., Deng, Z., Xiao, S., Yuan, B., Yang, K., 2019. How melittin inserts into cell membrane: conformational changes, inter-peptide cooperation, and disturbance on the membrane. Molecules 24 (1775), 1–17.

Hou, S., Liao, X., Kijlstra, A., Yang, P., 2020. Uveitis genetics. Exp. Eye Res. 190, 1–6. https://doi.org/10.1016/j.exer.2019.107853.

Hove, I.V., Lefevere, E., Groef, L.D., Sergeys, J., Salinas-Navarro, M., Libert, C., et al., 2016. MMP-3 deficiency alleviates endotoxin-induced acute inflammation in the posterior eye segment. Int. J. Mol. Sci. 17 (11), 1–23. https://doi.org/10.3390/ijms17111825.

Huang, X., Chau, Y., 2019. Intravitreal nanoparticles for retinal delivery. Drug Discov. Today 24 (8), 1510–1523. https://doi.org/10.1016/j.drudis.2019.05.005.

Huang, W., Collete III, W., Twamley, M., Aguirre, S.A., Sacaan, A., 2015. Application of electroretinography (ERG) in early drug development for assessing retinal toxicity in rats. Toxicol. Appl. Pharmacol. https://doi.org/10.1016/j.taap.2015.10.008.

ICCVAM, 2010. Test method evaluation report: current validation status of in vitro test methods proposed for identifying eye injury hazard potential of chemicals and products (volume 2. Interag. Coord. Comm. Validation Alternative Methods Natl. 2 (10).

Jung, W., Lee, C., Lee, D., Na, G., Lee, D., Choi, I., et al., 2014. The 15-deoxy-δ12,14-prostaglandin J2 inhibits LPS-stimulated inflammation via enhancement of the platelet-activating factor acetylhydrolase activity in human retinal pigment epithelial cells. Int. J. Mol. Med. 33, 449–456. https://doi.org/10.3892/ijmm.2013.1588.

Kim, W., An, H., Kim, J., Gwon, M., Gu, H., Sung, W.J., et al., 2017. Beneficial effects of melittin on ovalbumin-induced atopic dermatitis in mouse. Sci. Rep. 1–12. https://doi.org/10.1038/s41598-017-17873-2. December.

Lee, G., Bae, H., 2016. Anti-inflammatory applications of melittin, a major component of bee venom: detailed mechanism of action and adverse effects. Molecules 21 (5), 616.

Lee, R.W., Nicholson, L.B., Sen, H.N., Chan, C.C., Wei, L., Nussenblatt, R.B., et al., 2014. Autoimmune and autoinflammatory mechanisms in uveitis. Semin. Immunopathol. 36 (5), 581–594. https://doi.org/10.1007/s00281-014-0433-9.

Lehmann, J.S., Rughwani, P., Kolenovic, M., Ji, S., Sun, B., 2019. In: LEGENDplexTM: Bead-Assisted Multiplex Cytokine Profiling by Flow Cytometry, Methods in Enzymology, first ed., vol. 629. Elsevier Inc.

Leng, T., Miller, J.M., Bilbao, K.V., Palanker, D.V., Huie, P., Blumenkranz, M.S., 2004. The chick chorioallantoic membrane as a model tissue for surgical retinal research and simulation. Retina 24 (3), 427–434.

Leung, K.W., Barnstable, C.J., Tombran-tink, J., 2009. Bacterial endotoxin activates retinal pigment epithelial cells and induces their degeneration through IL-6 and IL-8 autocrine signaling. Mol. Immunol. 46, 1374–1386. https://doi.org/10.1016/j.molimm.2008.12.001.

Liang, C., Tai, M., Chang, Y., Chen, Y., Chen, C., Chien, M., et al., 2010. Glucosamine inhibits epidermal growth factor-induced proliferation and cell-cycle progression in retinal pigment epithelial cells. Mol. Vis. 16, 2559–2571.

Lin, L., Zhu, B., Cai, L., 2017. ScienceDirect Therapeutic effect of melittin on a rat model of chronic prostatitis induced by Complete Freund's Adjuvant. Biomed. Pharmacother. 90, 921–927. https://doi.org/10.1016/j.biopha.2017.04.055.

Liu, C.C., Hao, D., Zhang, Q., An, J., Zhao, J., Chen, B., et al., 2016. Application of bee venom and its main constituent melittin for cancer treatment. Cancer Chemother. Pharmacol. 78 (6), 1113–1130. https://doi.org/10.1007/s00280-016-3160-1.

Liu, H., Liu, W., Zhou, X., Long, C., Kuang, X., Hu, J., et al., 2017. Protective effect of lutein on ARPE-19 cells upon H 2 O 2 -induced G 2/M arrest. Mol. Med. Rep. 16, 2069–2074. https://doi.org/10.3892/mmr.2017.6838.

Maeda, H., Kawauchi, H., 1968. A new method for the determination of N-terminus of peptides chain with fluorescein-isothiocyanate. Biochem. Biophys. Res. Commun. 31 (2), 188–192.

Mai, K., Jjy, Chui, Girolamo, N.D., Mccluskey, P.J., Wakefield, D., 2014. Role of toll-like receptors in human iris pigment epithelial cells and their response to pathogen-

associated molecular patterns. J. Inflamm. 11 (1), 1–12. https://doi.org/10.1186/1476-9255-11-20.

Maugeri, A., Barchitta, M., Mazzone, M.G., Giuliano, F., Basile, G., Agodi, A., 2018. Resveratrol modulates SIRT1 and DNMT functions and restores LINE-1 methylation levels in ARPE-19 cells under oxidative stress and inflammation. Int. J. Mol. Sci. 19 (2118), 1–14. https://doi.org/10.3390/ijms19072118.

Mcclinton, K.J., Aliani, M., Kuny, S., Sauvé, Y., 2019. Differential effect of a carotenoid-rich diet on retina function in non-diabetic and diabetic rats. Nutr. Neurosci. 1–11. https://doi.org/10.1080/1028415X.2018.1563664.

Moon, D., Park, S., Lee, K., Heo, M., Kim, K., Kim, M., et al., 2007. Bee venom and melittin reduce proinflammatory mediators in lipopolysaccharide-stimulated BV2 microglia. Int. Immunopharm. 7, 1092–1101. https://doi.org/10.1016/j.intimp.2007.04.005.

Moreno, M., Giralt, E., 2015. Three valuable peptides from bee and wasp venoms for therapeutic and biotechnological use: melittin, apamin and mastoparan. Toxins 7, 1126–1150. https://doi.org/10.3390/toxins7041126.

Moschos, M.M., Gouliopoulos, N.S., Kalogeropoulos, C., 2014. Electrophysiological examination in uveitis: a review of the literature. Clin. Ophthalmol. 8, 199–214.

Nguyen, A.M., Rao, N.A., 2011. Oxidative photoreceptor cell damage in autoimmune uveitis. J. Ophthalmic Inflamm. Infect. 1 (1), 7–13. https://doi.org/10.1007/s12348-010-0007-5.

Onodera, H., Sasaki, S., Otake, S., Tomohiro, M., Shibuya, K., 2015. General considerations in ocular toxicity risk assessment from the toxicologists' viewpoints. J. Toxicol. Sci. 40 (3), 295–307.

Ozal, S.A., Turkekul, K., Gurlu, V., Guclu, H., Erdogan, S., 2018. Esculetin protects human retinal pigment epithelial cells from lipopolysaccharide-induced inflammation and cell death. Curr. Eye Res. 43 (9), 1169–1176. https://doi.org/10.1080/02713683.2018.1481517.

Paiva, MRB De, Vasconcelos-Santos, DV De, Coelho, M.M., MacHado, R.R., Lopes, N.P., Silva-Cunha, A., et al., 2021. Licarin A as a novel drug for inflammatory eye diseases. J. Ocul. Pharmacol. Therapeut. 37 (5), 290–300. https://doi.org/10.1089/jop.2020.0129.

Park, H.J., Son, D.J., Lee, C.W., Choi, M.S., Lee, U.S., Song, H.S., et al., 2007. Melittin inhibits inflammatory target gene expression and mediator generation via interaction with I k B kinase. Biochem. Pharmacol. 73, 237–247. https://doi.org/10.1016/j.bcp.2006.09.023.

Park, M.H., Choi, M.S., Kwak, D.H., Oh, K., Yoon, D.Y., Han, S.B., et al., 2011. anti-cancer effect of bee venom in prostate cancer cells through activation of caspase pathway via inactivation of NF- k B. Prostate 71, 801–812. https://doi.org/10.1002/pros.21296.

Park, J.-H., Kim, K.-H., Lee, W.-R., Han, S.-M., Park, K.-K., 2012. Protective effect of melittin on inflammation and apoptosis in acute liver failure. Apoptosis 17, 61–69. https://doi.org/10.1007/s10495-011-0659-0.

Pascoal, A., Manuela, M., Branco, A., Sousa-pimenta, M., 2019. An overview of the bioactive compounds, therapeutic properties and toxic effects of apitoxin. Food Chem. Toxicol. 134 (September), 110864. https://doi.org/10.1016/j.fct.2019.110864.

Rady, I., Siddiqui, I.A., Rady, M., Mukhtar, H., 2017. Melittin, a major peptide component of bee venom, and its conjugates in cancer therapy. Cancer Lett. 402, 16–31. https://doi.org/10.1016/j.canlet.2017.05.010.

Reddy, A., Fauziyya, M., Darren, J.L., 2018. Biological therapies that target inflammatory cytokines to treat uveitis. In: Advances in the Diagnosis and Management of Uveitis, p. 83.

Robson, A.G., Nilsson, J., Li, S., Jalali, S., Fulton, A.B., Patrizia, A., et al., 2018. ISCEV STANDARDS ISCEV guide to visual electrodiagnostic procedures. Doc. Ophthalmol. 136 (1), 1–26. https://doi.org/10.1007/s10633-017-9621-y.

Rosenbaum, J.T., Bodaghi, B., Couto, C., Zierhut, M., Acharya, N., Pavesio, C., et al., 2019. New observations and emerging ideas in diagnosis and management of non-infectious uveitis: a review. Semin. Arthritis Rheum. 49 (3), 438–445. https://doi.org/10.1016/j.semarthrit.2019.06.004.

Sabapathy, T., Deplazes, E., Manera, R., 2020. Revisiting the interaction of melittin with phospholipid bilayers: the effects of concentration and ionic strength. Int. J. Mol. Sci. 21 (746), 1–20.

Santos-Pinto, J.R.A., Perez-Riverol, A., Lasa, A.M., Palma, M.S., 2018. Diversity of peptidic and proteinaceous toxins from social Hymenoptera venoms. Toxicon 148, 172–196. https://doi.org/10.1016/j.toxicon.2018.04.029.

Saraswathy, S., Rao, A., 2008. Oxidative stress in experimental autoimmune uveitis. Ophthalmic Res. 40, 160–164. https://doi.org/10.1159/000119869.

Shibuya, K., Tomohiro, M., Sasaki, S., Otake, S., 2015. Characteristics of structures and lesions of the eye in laboratory animals used in toxicity studies. J. Toxicol. Pathol. 28, 181–188. https://doi.org/10.1293/tox.2015-0037.

Somwongin, S., Chantawannakul, P., Chaiyana, W., 2018. Toxicon Antioxidant activity and irritation property of venoms from Apis species. Toxicon 145, 32–39. https://doi.org/10.1016/j.toxicon.2018.02.049.

Son, D.J., Lee, J.W., Lee, Y.H., Song, H.S., Lee, C.K., Hong, J.T., 2007. Therapeutic application of anti-arthritis, pain-releasing, and anti-cancer effects of bee venom and its constituent compounds. Pharmacol. Ther. 115 (2), 246–270. https://doi.org/10.1016/j.pharmthera.2007.04.004.

Song, J., Han, D., Lee, H., Kim, D.J., Cho, J., 2020. A comprehensive proteomic and phosphoproteomic analysis of retinal pigment epithelium reveals multiple pathway alterations in response to the inflammatory stimuli. Int. J. Mol. Sci. 21 (3037), 1–18.

Srivastava, G.K., Alonso, M.L., Fernandez-Bueno, I., Maria, T., 2018. Comparison between direct contact and extract exposure methods for PFO cytotoxicity evaluation. Sci. Rep. 8, 1–9. https://doi.org/10.1038/s41598-018-19428-5.

Standardization of Uveitis Nomenclature (SUN) Working Group, 2005. Standardization of uveitis nomenclature for reporting clinical data. Results of the First International Workshop. Am. J. Ophthalmol. 140 (3), 509–516.

Taylor, A.W., Hsu, S., Ng, T.F., 2021. The role of retinal pigment epithelial cells in regulation of macrophages/microglial cells in retinal immunobiology. Front. Immunol. 12 (August), 1–10. https://doi.org/10.3389/fimmu.2021.724601.

Tipgomut, C., Wongprommoon, A., Takeo, E., Ittiudomrak, T., Puthong, S., Chanchao, C., 2018. Melittin induced G1 cell cycle arrest and apoptosis in Chago-k1 human bronchogenic carcinoma cells and inhibited the differentiation of THP-1 cells into tumour-associated macrophages. Asian Pac. J. Cancer Prev. APJCP 19, 3427–3434. https://doi.org/10.31557/APJCP.2018.19.12.3427.

Toledo, C.R., Pereira, V.V., Dourado, L.F.N., Paiva, M.R.B., Silva-Cunha, A., 2019. Corosolic acid: antiangiogenic activity and safety of intravitreal injection in rats' eyes. Doc. Ophthalmol. 138 (3), 181–194. https://doi.org/10.1007/s10633-019-09682-x.

Toledo, C.R., Paiva, M.R.B., Castro, B.F.M., Pereira, V.V., Cenachi, SP. de F., Vasconcelos-Santos, D.V., et al., 2021. Intravitreal lupeol: a new potential therapeutic strategy for noninfectious uveitis. Biomed. Pharmacother. 143 (July). https://doi.org/10.1016/j.biopha.2021.112145.

Usui, Y., Westenskow, P.D., Murinello, S., Dorrell, M.I., Scheppke, L., Bucher, F., et al., 2015. Angiogenesis and eye disease. Annu. Rev. Vis. Sci. 1, 155–184. https://doi.org/10.1146/annurev-vision-082114-035439.

Vieira, L.C., Moreira, C.P.D.S., Castro, B.F.M., Cotta, O.A.L., Silva, L.M., Fulgêncio, G.D.O., et al., 2020. Rosmarinic acid intravitreal implants: a new therapeutic approach for ocular neovascularization. Planta Med. 86 (17), 1286–1297. https://doi.org/10.1055/a-1223-2525.

Wehbe, R., Frangieh, J., Rima, M., Obeid, D El, Obeid, E., 2019. Bee venom: overview of main compounds and bioactivities for therapeutic interests. Molecules 24 (2997), 1–13. https://doi.org/10.3390/molecules24162997.

Yang, J.M., Yun, K.A., Jeon, J., Yang, H.Y., Kim, B., Jeong, S., et al., 2022. Multimodal evaluation of an interphotoreceptor retinoid-binding protein-induced mouse model of experimental autoimmune uveitis. Exp. Mol. Med. 54 (3), 252–262. https://doi.org/10.1038/s12276-022-00733-z.

Zhang, Z., Zhang, H., Peng, T., Li, D., Xu, J., 2016. Melittin suppresses cathepsin S-induced invasion and angiogenesis via blocking of the VEGF-A/VEGFR-2/MEK1/ERK1/2 pathway in human hepatocellular carcinoma. Oncol. Lett. 11, 610–618. https://doi.org/10.3892/ol.2015.3957.

Zhang, J., Zhou, K., Zhang, X., Zhou, Y., Li, Z., Shang, F., 2018. Celastrol ameliorates inflammation in human retinal pigment epithelial cells by suppressing NF-κB signaling. J. Ocul. Pharmacol. Therapeut. 35 (2), 1–8. https://doi.org/10.1089/jop.2018.0092.

Further reading

Chui, Jeanie J.Y., Li, Monique W.M., Girolamo, Nick Di, Chang, John H., McCluskey, Peter J., Wakefield, Denis, 2010. Iris Pigment Epithelial Cells Express a Functional Lipopolysaccharide Receptor Complex. Investig. Ophthalmol. Vis. Sci. 51, 2558–2567. https://doi.org/10.1167/iovs.09-3923.

Jamasbi, E, Mularski, A, Separovic, F, 2016. Model Membrane and Cell Studies of Antimicrobial Activity of Melittin Analogues. Curr. Top. Med. Chem. 16, 40–45.

Moon, D, Park, S, Lee, K, Heo, M, Kim, K, Kim, M, et al., 2007. Bee venom and melittin reduce proinflammatory mediators in lipopolysaccharide-stimulated BV2 microglia. Int. Immunopharm. 7, 1092–1101. https://doi.org/10.1016/j.intimp.2007.04.005.

Pereira, Ana Flavia Marques, Albano, Mariana, Alves, Fernanda Cristina Bergamo, Andrade, Bruna Fernanda Murbach Teles, Furlanetto, Alessandra, Rall, Vera Lucia Mores, et al., 2020. Influence of apitoxin and melittin from Apis mellifera bee on Staphylococcus aureus strains. Microb. Pathog. 141. https://doi.org/10.1016/j.micpath.2020.104011.